

First Session Adaptation: A Strong Replay-Free Baseline for Class-Incremental Learning

Aristeidis Panos
University of Cambridge

Yuriko Kobe
University of Cambridge

Daniel Olmeda Reino
Toyota Motor Europe

Rahaf Aljundi
Toyota Motor Europe

Richard E. Turner
University of Cambridge

Abstract

In Class-Incremental Learning (CIL) an image classification system is exposed to new classes in each learning session and must be updated incrementally. Methods approaching this problem have updated both the classification head and the feature extractor body at each session of CIL. In this work, we develop a baseline method, First Session Adaptation (FSA), that sheds light on the efficacy of existing CIL approaches, and allows us to assess the relative performance contributions from head and body adaption. FSA adapts a pre-trained neural network body only on the first learning session and fixes it thereafter; a head based on linear discriminant analysis (LDA), is then placed on top of the adapted body, allowing exact updates through CIL. FSA is replay-free i.e. it does not memorize examples from previous sessions of continual learning. To empirically motivate FSA, we first consider a diverse selection of 22 image-classification datasets, evaluating different heads and body adaptation techniques in high/low-shot offline settings. We find that the LDA head performs well and supports CIL out-of-the-box. We also find that Featurewise Layer Modulation (FiLM) adapters are highly effective in the few-shot setting, and full-body adaption in the high-shot setting. Second, we empirically investigate various CIL settings including high-shot CIL and few-shot CIL, including settings that have previously been used in the literature. We show that FSA significantly improves over the state-of-the-art in 15 of the 16 settings considered. FSA with FiLM adapters is especially performant in the few-shot setting. These results indicate that current approaches to continuous body adaptation are not working as expected. Finally, we propose a measure that can be applied to a set of unlabelled inputs which is predictive of the benefits of body adaptation.

1. Introduction

Continual learning (CL) is needed to bring machine learning models to many real-life applications. After a model is trained on a given set of data, and once deployed in its test environment, it is likely that new classes will naturally emerge. For example, in an autonomous driving scenario, new types of road transportation and traffic signage can be encountered. The deployed model needs to efficiently acquire this new knowledge with minimal cost (e.g. annotation requirements) without deteriorating the performance on existing classes of objects. The process of efficiently acquiring new knowledge while preserving what is already captured by the model is what continual learning methods target.

Continual learning can be mainly divided into task incremental learning and class incremental learning. Task incremental learning (TIL) sequentially learns independent sets of heterogeneous tasks and is out of this paper's scope. Class incremental learning (CIL), in contrast, assumes that all classes (already learnt and future ones) form part of a single classification task. In class-incremental learning, data arrive in a sequence of sessions with new classes appearing as the sessions progress. Critically, the data in each session cannot be stored in its entirety and cannot be revisited. The goal is to train a single classification model under these constraints.

In both task incremental and class incremental learning, the data distribution will change as the sessions progress. However, these changes tend to be smaller in real-world class incremental learning settings than in the task incremental setting. For, example consider a human support robot learning about new objects in a home in an incremental manner (CIL) vs. the same robot learning to adapt to different homes (TIL).

Practically, CIL has two major uses. First, in situations

where large amounts of data arrive in each session and so retraining the model is computationally prohibitive. Second, in situations where data are not allowed to be revisited due to privacy reasons such as under General Data Protection Regulation (GDPR). The latter situation is relevant for applications such as personalization where small numbers of data points are available i.e. few-shot continual learning. So-called replay-free methods are necessary for such settings, as samples of previous sessions are not allowed to be memorized, but CIL is known to be challenging in such settings.

Current SOTA methods for class incremental learning start from a pre-trained backbone [26, 35, 53, 52] and then adapt the features at each session of continual learning. The use of a pre-trained backbone has been shown to lead to strong performance especially in the few-shot CIL setting due to the lack of data [38]. However, it is unclear to what extent continuous adaption of the features in each session is helpful. In general, in CIL there is a trade-off between adaptation (which helps adapt to the new statistics of the target domain) and catastrophic forgetting (whereby earlier classes are forgotten as the representation changes). When memorization of previous samples is restricted, the benefits from adapting the feature extractor body to learn better features might well be out-weighted by the increase in forgetting of old classes. Moreover, body adaptation in earlier sessions is arguably more critical (e.g. adapting the backbone to the new domain in the first session), whilst it is less essential in later sessions where the changes in the ideal representation between sessions are smaller.

This work explores under what conditions continuous adaptation of the body is beneficial, both in principle and in current practice. In order to do this, we develop a new replay-free method, inspired by the first encoding method of [2], called First Session Adaptation (FSA). FSA adapts the body of a pre-trained neural network on only the first session of continual learning. We investigate adapting all body parameters and the use of Feature-wise Layer Modulation (FiLM) adapters [40] which learn only a small number of parameters. The head, in contrast, is adapted at each session using an approach that is similar to Linear Discriminate Analysis (LDA), which suffers from no forgetting, and improves over the Nearest Class Mean classifier (NCM) [32] approach. The efficacy of this general approach, including comparisons to a standard linear head, is first motivated through experiments in the offline setting (Sec. 4.2). We then carry out experiments under three CIL settings. First, we consider the high-shot setting (high-shot CIL). The other two settings consider few-shot continual learning. Specifically, one setting follows previous approaches that employ an initial session with a large number of data points and few-shot sessions thereafter (few-shot+ CIL) while the other exclusively includes sessions with only a small amount of data

(few-shot CIL).

The contributions of the paper are as follows: (1) We develop a replay-free CIL baseline, namely FSA, that is extremely simple to implement and performs well in many different scenarios. (2) We empirically motivate FSA through a set of offline experiments that evaluate different forms of neural network head and body adaptation; (3) We then compare FSA to a set of strong continual learning baseline methods in a fair way using the same pre-trained backbone for all methods. (4) We show that the FSA-FiLM baseline performs well in the high-shot CIL setting, outperforming the SOTA whilst avoiding data memorization. (5) In the few-shot learning settings, FSA outperforms existing continual learning methods on eight benchmarks, often by a substantial margin, and is statistically tied with the best performing method on the one remaining dataset. (6) Finally, we propose a measure that can be applied to a set of unlabelled inputs which is predictive of the benefits of body adaptation.

2. Related Work

Class Incremental Learning is more challenging than task-incremental continual learning as a shared output layer is used for the classes of different learning sessions. We refer to [10] for a survey on both class and task incremental learning. While softmax cross entropy loss is considered a standard in classification models, it is shown to be a source of class interference in continual learning [56, 5]. Thus, recent works either focus on fixing the softmax classifier [5, 1, 63] or deploy nearest class mean classifiers (NCM) as an alternative [42, 8, 21]. In this work, we deploy an LDA classifier that uses the mean embedding of each class and an incrementally updated covariance matrix shared across all classes. We show that this approach is comparable to a softmax classifier in the offline setting and that it outperforms NCM.

Due to the challenging nature of class incremental learning, some methods employ a buffer of stored samples from previous sessions [41, 58]. [41] suggests a simple baseline, GDumb, that performs offline training on both buffer data and new session data at each incremental step. GDumb shows strong performance compared to sophisticated continual learning solutions. Here we show that our simple yet effective solution often outperforms variants of GDumb that have a large memory without leveraging any buffer of stored samples.

In addition to the issues arising from the shared classification layer, learning a feature extractor that can provide representative features of all classes is a key element in continual learning. Some class incremental learning methods leverage large initial training session or start from a pre-trained network, e.g., [53, 16, 54] and show improved overall continual learning performance without questioning the

role of such pre-training steps and whether the learned representations have in fact improved. Recently, [35] studies continual learning with strong pre-trained models and proposes deploying exemplar-based replay in the latent space using a small multilayer network on top of the fixed pre-trained model. The authors show that such latent replay improves performance, especially for tasks that are different from the distribution used to train the initial model. In this work, we show that adaptation of pre-trained models is essential for strong continual learning performance. However, different from all existing continual learning works, we show that adapting the representation only in the first session is sufficient to obtain representative features for the classes being learned and that this forms a strong baseline for future continual learning methods.

In addition to the incremental classification in the full data regime, we focus on the few-shot scenario where only a few labeled examples per class are provided at each training session. [16] utilize a meta-trained network for few-shot classification and explore multiple design choices including a no-adaptation baseline and a method to optimize orthogonal prototypes with the last classification layer only. The method heavily relies on a pre-training and meta-training step on a large subset of classes from the original dataset. In this work, we show that the meta-training step is not essential and that a simple LDA head is sufficient without the reliance on a big initial training stage. In [21] the authors propose a new distillation loss functioning at the feature map level where importance values are estimated per feature map along with replay and consider an NCM classifier at test time. [64] heavily relies on the training of an initial session using a specific loss function that takes into account classes that will be added in future. It further requires that the total number of classes to be known *a priori* which is unrealistic for real applications. Our solution adapts FiLM parameters to the first session data and fixes the representation for the remaining training sessions. We show that surprisingly few samples in the first session are sufficient for adaptation and that our solution is more powerful than current few-shot continual learning solutions.

Finally, the LDA head has been also utilized for CIL in [13]. However, in [13] a slightly different regularized covariance matrix was used and the pre-trained feature extractor was frozen across sessions without fine-tuning at all. As we show in our experiments, this strategy is sub-optimal and fine-tuning the FiLM parameters offers a significant performance boost.

3. Proposed Algorithm

In this section, first we discuss the main components of the proposed methods FSA/FSA-FiLM, namely body adaptation techniques and classifier heads. Then we formally introduce the two methods for tackling CIL.

3.1. Problem Formulation

In CIL, we are given a dataset $\mathcal{D}_s = \{\mathbf{x}_{i,s}, y_{i,s}\}_{i=1}^{N_s}$ for each session $s \in \{1, \dots, S\}$, where $X_s = \{\mathbf{x}_{i,s}\}_{i=1}^{N_s}$ is a set of images and $Y_s = \{y_{i,s}\}_{i=1}^{N_s}$ is the set of the corresponding labels with $y_{i,s} \in \mathcal{Y}_s$. Here \mathcal{Y}_s is the label space of session s . It is common in CIL that label spaces are mutually exclusive across sessions, i.e. $\mathcal{Y}_s \cap \mathcal{Y}_{s'} = \emptyset, \forall s \neq s'$ and we only have access to \mathcal{D}_s in the current session s to train our model. The proposed FSA method can naturally handle sessions with overlapping label spaces too, however, we follow the former paradigm in our experiments. Another typical assumption in CIL is that the data in all sessions come from the same dataset. We also adopt this assumption in this work, although our experiments on DomainNet are a step toward considering different datasets in each session.

In session s , we will use models defined as

$$f_s(\mathbf{x}) = W_s^\top g_{\theta_s}(\mathbf{x}) + \mathbf{b}_s, \quad (1)$$

where $g_{\theta_s}(\mathbf{x}) \in \mathbb{R}^d$ is a feature extractor backbone¹ with session-dependent parameters θ_s . The linear classifier head comprises the class weights $W_s \in \mathbb{R}^{d \times |\mathcal{Y}_{1:s}|}$ and biases $\mathbf{b}_s \in \mathbb{R}^{|\mathcal{Y}_{1:s}|}$, and $\mathcal{Y}_{1:s} = \cup_{j=1}^s \mathcal{Y}_j$ is the label space of all distinct classes we have seen up to session s . Ideally, when a new dataset \mathcal{D}_s is available at the s -th session, the model should be able to update the backbone parameters θ and the linear classifier head W_s with the minimum computational overhead and without compromising performance over the previously seen classes $\mathcal{Y}_{1:s}$.

Backbone adaptation. Traditionally, the adaptation of the body at the current session s requires updating the full set of the network parameters θ_s (full-body adaptation). Options include using specifically designed loss functions that mitigate catastrophic forgetting or using a memory buffer that stores a subset of the previously encountered data. See [29] for a review of continual learning techniques. Nevertheless, when training data availability is scarce relative to the size of the model then full-body adaptation ceases to be suitable, and few-shot learning techniques [51], such as meta-learning [18] and transfer learning [59] become favorable.

Recent works in few-shot learning [43] showed that a pre-trained backbone can be efficiently adapted by keeping its parameters θ_s frozen and introducing Feature-wise Linear Modulation (FiLM) [40] layers with additional parameters ξ_s which scale and shift the activations produced by a convolutional layer. In [43], these parameters are generated by a meta-trained network when a downstream task is given. Alternatively, ξ_s can be learned (fine-tuned) by the downstream data as in [44]. In this work, we consider both

¹In this paper, we interchangeably use the terms feature extractor, backbone, and body.

meta-learned (Supplement) and fine-tuned (Sec. 4) FiLM parameters.

Classifier heads. In both offline and CIL settings, (linear) classifier heads can be divided into two groups; parametrized and parameter-free. Parametrized heads require the weights/biases in Eq. (1) to be updated by an iterative gradient-based procedure whilst for parameter-free heads, a closed-form formula is available that directly computes the weights/biases after the update of the backbone. We consider three different heads (for notational simplicity we consider the offline setting, and thus suppress session s dependence), one parametrized, and two parameter-free.

- The linear (learnable) head where W, \mathbf{b} are learned.
- The Nearest Class Mean (NCM) classifier where the weight and bias of the k -th class is given by

$$\mathbf{w}_k = \hat{\boldsymbol{\mu}}_k \text{ and } b_k = \ln \frac{|X^{(k)}|}{N} - \frac{1}{2} \hat{\boldsymbol{\mu}}_k^\top \hat{\boldsymbol{\mu}}_k, \quad (2)$$

where $X^{(k)} = \{\mathbf{x}_i : y_i = k\}$ is the set of images belonging in class k and $\hat{\boldsymbol{\mu}}_k = \frac{1}{|X^{(k)}|} \sum_{\mathbf{x} \in X^{(k)}} g_{\boldsymbol{\theta}}(\mathbf{x})$ is the mean vector of the embedded images of class k .

- The Linear Discriminant Analysis (LDA) classifier with weights/biases defined as

$$\mathbf{w}_k = \tilde{S}^{-1} \hat{\boldsymbol{\mu}}_k \text{ and } b_k = \ln \frac{|X^{(k)}|}{N} - \frac{1}{2} \hat{\boldsymbol{\mu}}_k^\top \tilde{S}^{-1} \hat{\boldsymbol{\mu}}_k, \quad (3)$$

where $\tilde{S} = S + I_d$ is the regularized sample covariance matrix with sample covariance matrix $S = \frac{1}{|X|-1} \sum_{\mathbf{x} \in X} (g_{\boldsymbol{\theta}}(\mathbf{x}) - \hat{\boldsymbol{\mu}})(g_{\boldsymbol{\theta}}(\mathbf{x}) - \hat{\boldsymbol{\mu}})^\top$, $\hat{\boldsymbol{\mu}} = \frac{1}{|X|} \sum_{\mathbf{x} \in X} g_{\boldsymbol{\theta}}(\mathbf{x})$, and identity matrix $I_d \in \mathbb{R}^{d \times d}$.

Both NCM and LDA classifiers are suitable for CIL since their closed-form updates in Eq. (2) and Eq. (3) support exact, computationally inexpensive, continual updates (via running averages) that incur no forgetting. Updating the linear head, in contrast, requires more computational effort and machinery when novel classes appear in a new session. Notice that setting $\tilde{S} = I_d$ in LDA recovers NCM.

The continuous update of the LDA head is not as straightforward as it is for NCM, since LDA also requires updating the sample covariance S . We discuss how this can be attained in the next section where we introduce our proposed method FSA/FSA-FiLM.

3.2. First Session Adaptation

Motivated by the efficient adaptation techniques and CIL-friendly classifiers discussed in the previous section, we propose two simple and computationally efficient CIL

methods called First Session Adaptation (FSA) and FSA-FiLM. FSA is based on a full-body adaptation while FSA-FiLM uses FiLM layers to adapt the body. Both methods utilize pre-trained backbones. FSA (-FiLM) (i) adapts the backbone only at the first session and then the backbone remains frozen for the rest of the sessions, and (ii) makes use of an LDA classifier which is continuously updated as new data become available. For adapting the body (either full or FiLM-based adaptation) at the first session, we use a linear head and a cross-entropy loss first, and then after the optimization is over, the linear head is removed and an LDA head is deployed instead, based on the optimized parameters $\boldsymbol{\theta}^*$ and Eq. (3). Updating the LDA head when the data of the next session becomes available, can be done by using Algorithm 1 recursively until the last session S . Specifically, by having access to the running terms $\{A, \mathbf{b}, \text{count}\}$, the sample covariance matrix is given by

$$S = \frac{1}{\text{count} - 1} \left(A - \frac{1}{\text{count}} \mathbf{b} \mathbf{b}^\top \right). \quad (4)$$

The time complexity of LDA scales as $\mathcal{O}(d^3 + |\mathcal{Y}_s|d^2)$ and

Algorithm 1 Update of sample covariance running terms

Require: $g(\cdot) \equiv$ a feature extractor backbone

Require: $X_s = \{\mathbf{x}_{i,s}\}_{i=1}^{N_s}$: Images of session s

Require: $A \in \mathbb{R}^{d \times d}$, $\mathbf{b} \in \mathbb{R}^d$, $\text{count} \in \mathbb{N}^*$ if $s > 1$

- 1: **function** INCUPDATE($g(\cdot), X_s, A, \mathbf{b}, \text{count}$)
 - 2: **if** $s = 1$ **then** ▷ Initialize $A, \mathbf{b}, \text{count}$
 - 3: $A \leftarrow \mathbf{0}_{d \times d}, \mathbf{b} \leftarrow \mathbf{0}_d, \text{count} \leftarrow 0$
 - 4: **end if**
 - 5: $A \leftarrow A + \sum_{\mathbf{x} \in X_s} g(\mathbf{x})g(\mathbf{x})^\top$
 - 6: $\mathbf{b} \leftarrow \mathbf{b} + \sum_{\mathbf{x} \in X_s} g(\mathbf{x})$
 - 7: $\text{count} \leftarrow \text{count} + N_s$
 - 8: **return** $A, \mathbf{b}, \text{count}$
 - 9: **end function**
-

its space complexity is $\mathcal{O}(d^2 + |\mathcal{Y}_{1:s}|d)$ at the s -th session. This computational burden is negligible compared to taking gradient steps for learning a linear head and as we will see in Sec. 4.2 using covariance information boosts performance significantly against the vanilla NCM head.

4. Experiments

In this section, we present a series of experiments to investigate the performance of FSA (-FiLM) under different CIL settings. First, we detail the datasets used for the experiments and discuss our implementation. Second, we perform a large empirical comparison between LDA, linear, and NCM classifiers, in combination with different body adaptation techniques, in the offline setting. For the CIL settings, the results are compared to the vanilla method, *No Adaptation (NA)*, where a pretrained backbone is combined

with an LDA head and remains frozen across sessions. We also consider how these findings are affected by the number of shots available. Third, we compare FSA (-FiLM) with state-of-the-art continual learning methods and conduct ablation studies. Finally, we investigate the effect of adapting the backbone when the CIL dataset is “similar” to ImageNet-1k and discuss a similarity metric that indicates whether body adaptation is required.

4.1. Datasets and Implementation details

Datasets. We employ a diverse collection of 26 image-classification datasets across the offline and CIL experiments. For the offline experiments of Sec. 4.2, we use the 19 datasets of VTAB [61], a low-shot transfer learning benchmark, plus three additional datasets, FGVC-Aircraft [30], Stanford Cars [23], and Letters [9]. We refer to this group of datasets as VTAB+. For the CIL-based experiments, we choose 5 VTAB+ datasets from different domains, having an adequate number of classes to create realistic CIL scenarios. The datasets are CIFAR100, SVHN, dSprites-location, FGVC-Aircraft, Cars, and Letters while also including 4 extra datasets: CUB200 [50], CORE50 [28], iNaturalist [47], and DomainNet [39]. Exact details for each dataset are provided in the Supplement.

Training details. All models are implemented with PyTorch [37]. We use a pre-trained EfficientNet-B0 [45] on Imagenet-1k as the main backbone for all methods. For the few-shot+ CIL experiment in Sec. 4.3, we also consider two ResNet architectures, ResNet-18 and ResNet-20 [14] to enable direct comparison to the original settings used in [64]. All the deployed backbones (except ResNet-20, due to the unavailability of pre-trained weights on ImageNet-1k), are pre-trained on ImageNet-1k for all methods. We keep the optimization settings the same across all baselines for fairness. Optimization details are given in the Supplement.

Evaluation protocol. We report the Top-1 accuracy after the last continual learning session evaluated on a test set including instances from all the previously seen classes. In the Supplement, we provide the accuracy after each session. To quantify the forgetting behavior, we use a scaled modification of the performance dropping rate [46], namely percent performance dropping rate (PPDR), defined as $PPDR = 100 \times \frac{\mathcal{A}_1 - \mathcal{A}_S}{\mathcal{A}_1} \%$, where \mathcal{A}_1 denotes test accuracy after the first session, and \mathcal{A}_S the test accuracy after the last session.

4.2. Head Comparisons

To motivate the choice of the LDA head for FSA (-FiLM), we compare its average accuracy across all VTAB+ datasets with that of the linear and NCM classifiers under the *offline* setting where all the classes are available and no incremental learning is required. For the body, we use

no adaptation (NA) as a baseline (i.e. using the unadapted original backbone), FiLM-based adaptation, and full-body adaptation while ranging the number of shots from 5 to 10, then 50, and finally using all available training data. As Fig. 1 illustrates, LDA consistently outperforms both NCM and linear heads when the number of shots is equal to 5 and 10, regardless of adaptation technique. Notice also that as the number of learnable parameters increases, the choice of the head plays a less significant role in the predictive power of the method. Overall, LDA performs similarly to the linear head in the high-shot settings and performs the best of all heads in the low-shot settings. Finally, the full covariance information of LDA provides a consistent advantage over its isotropic covariance counterpart, i.e. the NCM classifier. This is in agreement with the results presented in [44] for the LDA and NCM classifier. In addition to the results presented here, we have also tested meta-learning based body adaptation methods [4, 43, 2] which support continual learning out of the box. We find these perform poorly compared to the fine-tuning based methods. See next section for more results.

4.3. Class-Incremental Learning Comparisons

We consider three different CIL scenarios: (i) high-shot CIL, (ii) few-shot+ CIL, and (iii) few-shot CIL. We compare our FSA/FSA-FiLM methods with recent state-of-the-art FSCIL methods, including Decoupled-Cosine [49], CEC [62], FACT [64], and ALICE. Additionally, for the high-shot CIL setting, we consider a strong replay-based baseline for CIL, GDumb [41] and a competitive replay-free method, E-EWC+SDC [60]. Finally, we introduce an additional baseline adapter inspired by [55], called FSA-LL (Last Layer). In FSA-LL only the parameters of the backbone’s last block are fine-tuned which can be compared to the FSA-FiLM adaption method.

High-shot CIL. In this setting, we consider all the available training data for each class while keeping the number of novel classes in each session low. We use CIFAR100, CORE50, SVHN, dSprites-loc, FGVC-Aircraft, Cars, and Letters for our experiments. For CIFAR100, CORE50, and FGVC-Aircraft, the first session consists of 10 classes, 4 for dSprites-loc, 16 for Cars, and 12 for letters. The rest of the sessions include 10 classes for CIFAR100, FGVC-Aircraft, 20 for Cars, 5 for CORE50 and Letters, 2 for SVHN and dSprites-loc. Therefore, the total number of incremental sessions for CIFAR100, FGVC-Aircraft, and Cars is 10 while for CORE50 we have 9 sessions. A pre-trained on Imagenet-1k EfficientNet-B0 is deployed as a backbone for all methods. FSA-FiLM outperforms all the competitors by a significant margin on all datasets except dSprites-loc. We attribute the performance gap on dSprites-loc due to the large number of data points (25k) and the portion of the

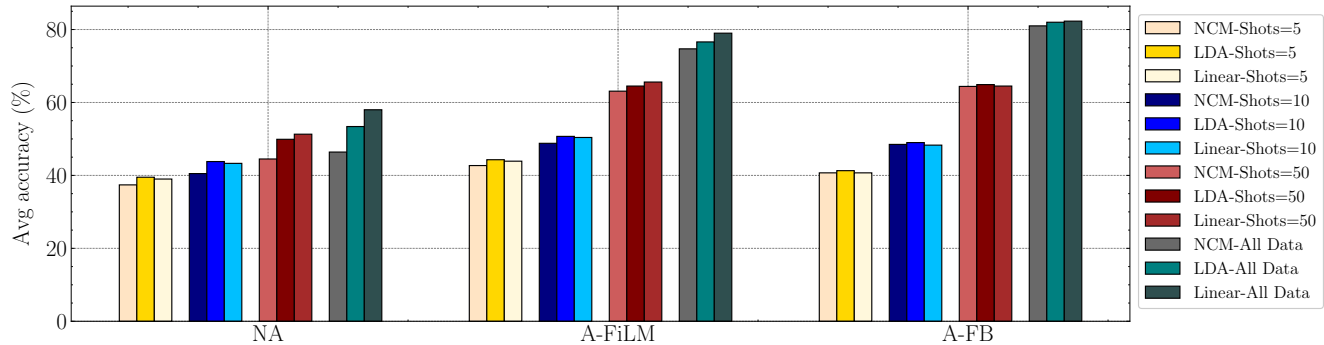


Figure 1. Average accuracy across all VTAB+ datasets using no-adaptation (NA), FiLM adaptation (A-FiLM), and full body adaptation (A-FB) for different classifier heads (NCM, LDA, Linear) and number of shots (5, 10, 50, All Data). The results correspond to the offline setting where all classes are available without any incremental learning.

Method	CIFAR100	CORE50	SVHN	dSprites-loc	FGVC-Aircraft	Cars	Letters	Avg Diff
NA	68.2 (26.8)	82.6 (14.2)	39.9 (51.1)	20.6 (54.0)	41.3 (1.7)	43.3 (40.3)	68.4 (24.1)	0.0
E-EWC+SDC [60]	32.4 (66.7)	21.7 (78.1)	39.5 (60.1)	18.6 (81.4)	25.6 (55.8)	30.0 (62.6)	33.6 (66.3)	-23.3
FACT [64]	10.2 (89.4)	22.0 (77.7)	33.8 (65.9)	6.4 (93.6)	4.7 (90.3)	0.6 (99.3)	20.9 (79.1)	-38.0
ALICE [38]	52.4 (45.8)	72.8 (25.8)	46.1 (53.6)	68.3 (31.7)	39.8 (35.0)	36.4 (56.0)	75.7 (24.2)	+3.9
FSA	62.8 (34.5)	82.8 (15.5)	71.3 (26.6)	91.5 (8.5)	50.8 (6.3)	50.3 (36.6)	78.4 (21.4)	+17.7
FSA-LL	60.5 (37.2)	79.0 (19.2)	64.6 (33.1)	91.3 (8.5)	45.4 (21.7)	45.7 (43.8)	77.2 (22.7)	+14.2
FSA-FiLM	73.8 (23.4)	85.4 (13.3)	75.9 (23.4)	76.9 (22.8)	55.9 (-5.7)	55.9 (30.2)	79.7 (20.0)	+19.9
GDumb [41]	54.5 (42.2)	82.4 (15.0)	78.2 (19.6)	79.5 (12.9)	25.3 (56.9)	14.2 (82.6)	70.1 (27.0)	+5.7
Offline-FiLM	78.2	88.4	93.1	98.5	67.5	67.3	85.2	+30.6

Table 1. Last session’s test accuracy (%) (\uparrow) and the PPDR (%) (\downarrow) in parentheses, for the high-shot CIL setting (Sec. 4.3). The last column reports the average accuracy difference (\uparrow) across all datasets between a baseline and NA. A pre-trained EfficientNet-B0 on Imagenet-1k is used as a backbone for all methods. For reference, we include the replay-based baseline GDumb where 1k images are used for the memory buffer.

classes (25%) in the first session. It is also apparent the efficiency of fine-tuning FiLM parameters over fine-tuning the parameters of the model’s last layer; note the number of FiLM parameters is only 20.5k while the last layer of an EfficientNet-B0 comprises 2.9M parameters. Furthermore, fine-tuning the FiLM parameters offer almost 20% accuracy increase on average compared to using a pretrained model without doing any further adaptation. Interestingly, the replay-free FSA-FiLM is able to outperform significantly the replay-based method GDumb with a 1k memory buffer on most of the datasets; accuracy and time comparisons between FSA-FiLM and GDumb with varying buffer sizes can be found in Figure 1 of the Appendix. Regarding FACT’s performance, although it starts from a pre-trained backbone, it was developed under the assumption that the first session contains lots of data and a high fraction of the classes that will be encountered ($> 50\%$) which is not true for the setting treated in Table 1. FACT overfits in this setting and this results in poor performance. It turns out that FACT’s assumptions about the first session are a strong requirement which is not necessary for obtaining good performance as

our FSA baseline shows.

Few-shot+ CIL. This setting is the one that has most commonly been used for few-shot CIL (FSCIL) and it involves an initial session that contains a large number of classes (around 50-60% of the total number of classes in the dataset) and all the available training images of these classes. The remaining sessions comprise a small number of classes and shots (typically 5/10-way 5-shot). Here we follow the exact FSCIL settings as described in [64, 38] for CIFAR100 and CUB200. We use ResNet-18/20 and EfficientNet-B0 as backbones. Table 2 summarizes the performance comparison between baselines. FSA performs on par with FACT on CIFAR100 when we use the original backbone used in [64], and it outperforms FACT by almost 10% and ALICE by 3.4% when EfficientNet-B0 is utilized while FSA-FiLM exhibits the lowest PPDR score. Notice also that FSA is only marginally worse than its offline counterpart, meaning there is little room for continuous body adaptation to improve things further. For CUB200, FSA with an EfficientNet-B0 performs on par with ALICE. Inter-

estingly, we observe that NA performs well on this dataset. This indicates that CUB200 is not far from ImageNet-1k. The current results of FSA set new SOTA performance on CIFAR100 for the FSCIL setting.

Method	Backbone	Datasets	
		CIFAR100	CUB200
CEC [62]		49.1 (32.7)*	-
FACT [64]	RN-20	52.1 (30.2)*	-
FSA		52.0 (30.8)	-
NA		50.4 (26.8)	50.0 (29.3)
CEC [62]		-	52.3 (31.1)*
FACT [64]	RN-18	49.5 (34.8)*	56.9 (25.0)*
ALICE [38]		54.1 (31.5) [†]	60.1 (22.4) [†]
FSA-FiLM		55.2 (24.4)	52.7 (27.6)
FSA		61.4 (25.1)	57.6 (24.3)
NA		55.2 (25.8)	63.2 (19.6)
FACT [64]		56.5 (34.6)	62.9 (23.3)
ALICE [38]	EN-B0	62.7 (28.4)	63.5 (22.2)
FSA-LL		61.4 (25.7)	55.9 (22.3)
FSA-FiLM		61.8 (22.4)	62.9 (20.4)
FSA		66.1 (24.6)	63.4 (20.9)
Offline	EN-B0	67.0	65.1

Table 2. Baseline comparison under the few-shot+ CIL setting (Sec. 4.3). We report the accuracy (%) ([†]) of the last session and the PPDR (%) (_↓) in parentheses. Asterisk (*) indicates that the reported results are from [64] and [†] indicates results reported in [38]. We use three different backbones, EfficientNet-B0 (EN-B0) and ResNet-18/20 (RN-18/20); EN-B0 and RN-18 are pre-trained on Imagenet-1k.

Few-shot CIL. The final setting, which is firstly introduced in this work, considers an alternative FSCIL setting in which only a small number of data points are available in all sessions, including the first. We use 50 shots per session while the first session includes 20% of the total number of classes of the dataset. Each of the remaining sessions includes around 10% of the total number of classes; more details are available in the Supplement. We repeat experiments 5 times and we report the mean accuracy and PPDR in Table 3. FSA-FiLM outperforms all the other baselines by a large margin in terms of both accuracy and PPDR, indicating that transfer learning is considerably advantageous for CIL when the data availability is low. Notice that both ALICE and FACT struggle to achieve good performance under this setting due to the limited amount of data in the first session. We find that FGVC-Aircraft exhibits a positive backward transfer behavior that we attribute to a difficult initial session followed by sessions that contain classes that are comparatively easier to distinguish.

Finally, we demonstrate the suitability of the LDA head in FSA-FiLM compared to a nearest class mean head, de-

noted FSA-FiLM-NCM. In the continual learning setting, LDA gives far larger improvements over NCM; e.g. 10% on average as presented in Table 3. This highlights the importance of a strong classification layer. Note that the incremental update of LDA does not require any replay buffer as opposed to a linear head.

4.4. Inhomogeneous Class-Incremental Learning

FSA adapts the body only on the first session of continual learning and it is therefore likely to be sensitive to the particular classes which are present in this session. To investigate the degree of performance sensitivity for FSA, we devise a setting similar to the few-shot CIL setting of Sec. 4.3, where each session includes classes that share some common attribute. We select CIFAR100 which provides super-class information, and DomainNet which consists of different domains and also has superclass information available. We create three distinct CIL configurations for each dataset, each of which has different types of data in the first session. For CIFAR100, we split the data into 19 sessions. The first session includes 10 classes from super-classes (i) aquatic mammals and fish (*Aq*), (ii) electric devices and furniture (*DevF*), or (iii) Vehicles 1 and Vehicles 2 (*Veh*). Each of the other 18 sessions include images from the remaining 18 super-classes. Similarly, for DomainNet, we split the data into 6 sessions using 50 shots with 10 classes in each session. The first session includes 10 classes of (i) the “electricity” superclass of the real domain (*El-R*), (ii) the “furniture” superclass of the clipart domain (*F-Clp*), or (iii) the “transportation” superclass of the sketch domain (*Tr-Sk*). In this way, we can vary the content of the first session and analyze the effect this has on performance. Table 4 reveals that FSA-FiLM’s performance is similar even if the data in the first session used for the body adaptation appears disparate from that contained in the remaining sessions. Even for DomainNet where the distribution shift of the data across sessions is considerable, performance is only marginally affected in each of the three settings. This provides evidence that adapting the body only on the first session achieves competitive performance regardless of the class order, given the assumption that the data come from a single dataset (albeit a varied one in the case of DomainNet).

4.5. When to adapt the body?

Despite the strong performance of FSA (-FiLM) in the few-shot settings of Sec. 4.3, there are cases where the NA method achieves very close accuracy to FSA (e.g. see CUB200 results in Table 2). This implies that there may be datasets where adaptation is not required and all we need is the pre-trained backbone. In order to decide whether we require body adaptation or not, we compute the minimum cosine distance in the embedding space of the pre-trained backbone between the downstream dataset and the

Method/Dataset	CIFAR100	SVHN	dSprites-loc	FGVC-Aircraft	Letters	DomainNet	iNaturalist	Avg Diff
NA	57.4 (28.4)	28.3 (61.5)	11.9 (66.6)	41.0 (-15.5)	57.6 (29.9)	69.0 (17.2)	49.7 (4.3)	0.0
FACT [64]	16.8 (79.7)	24.1 (66.2)	11.7 (64.1)	8.3 (79.9)	49.8 (40.9)	20.6 (75.6)	14.3 (74.0)	-24.2
ALICE [38]	58.0 (33.8)	23.0 (65.9)	23.0 (46.0)	42.0 (27.5)	66.5 (31.4)	66.5 (25.1)	47.9 (13.7)	+1.7
FSA	60.3 (27.0)	32.9 (53.5)	33.7 (41.3)	50.1 (-16.8)	62.2 (28.5)	70.3 (17.5)	51.5 (1.1)	+6.6
FSA-LL	62.0 (25.7)	43.5 (47.0)	18.8 (61.7)	45.8 (-2.1)	69.4 (26.1)	67.6 (16.9)	49.2 (14.1)	+5.9
FSA-FiLM-NCM	66.4 (24.8)	38.8 (56.5)	25.1 (59.4)	42.5 (-7.5)	57.1 (34.9)	68.8 (18.5)	51.5 (12.1)	+5.0
FSA-FiLM	70.9 (20.5)	51.3 (43.5)	35.7 (43.1)	55.8 (-19.8)	73.4 (22.1)	74.0 (15.6)	58.8 (4.8)	+15.0
Offline-FiLM	73.8	77.2	83.7	65.1	79.7	75.1	62.1	+28.0

Table 3. Accuracy (%) (\uparrow) of the last session and PPDR (%) (\downarrow) in parentheses for the few-shot CIL setting of Sec. 4.3. The last column reports the average accuracy difference (\uparrow) across all datasets between a baseline and NA. A pre-trained EfficientNet-B0 on ImageNet-1k is used as a backbone for all methods. FSA-FiLM-NCM utilizes an NCM classifier while NA, FSA (-LL, FiLM) and Offline uses an LDA head.

Dataset	NA	Aq	DevF	Veh
CIFAR100	57.4 \pm 1.0	66.1 \pm 1.6	66.2 \pm 1.9	67.9 \pm 1.2
	NA	El-R	F-Clp	Tr-Sk
DomainNet	69.0 \pm 0.4	70.6 \pm 0.6	71.7 \pm 0.6	72.8 \pm 0.5

Table 4. Last session accuracy (%) (\uparrow) of FSA-FiLM for three different session splits on CIFAR100 and DomainNet as described in Sec. 4.4. For reference, we also include the accuracy of NA. Results are averaged over 5 runs (mean \pm std).

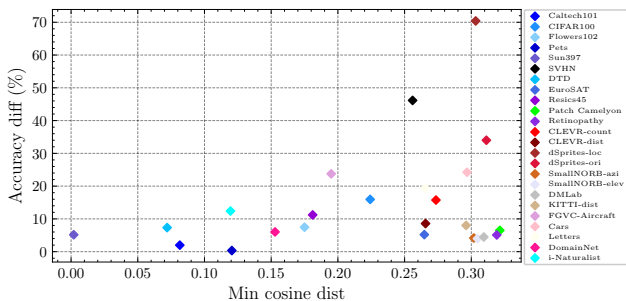


Figure 2. Scatter plot of the accuracy differences between FSA-FiLM and NA against the minimum cosine distance between a dataset and *miniImagenet* dataset evaluated using the NA method. We consider the offline setting with 50 shots. A pre-trained EfficientNet-B0 on ImageNet-1k is used as a backbone.

miniImagenet [49] dataset. We use *miniImagenet* (60k images) as a proxy of Imagenet-1k (1.3M images) to reduce the computational overhead of evaluating pairwise distances. This allows us to approximately measure the dissimilarity between the downstream dataset and Imagenet-1k.

Fig. 2 shows the accuracy difference between FSA-FiLM and NA as a function of the cosine distance for the offline setting with 50 shots whilst Fig. 3 illustrates the same accuracy difference where the datasets are grouped based on the VTAB+ categorization. For this experiment, we use 24 datasets (VTAB+, DomainNet, and iNaturalist). We ob-

serve that adaptation is more beneficial for datasets in the structured domain, which contain images that are dissimilar to those of ImageNet-1k.

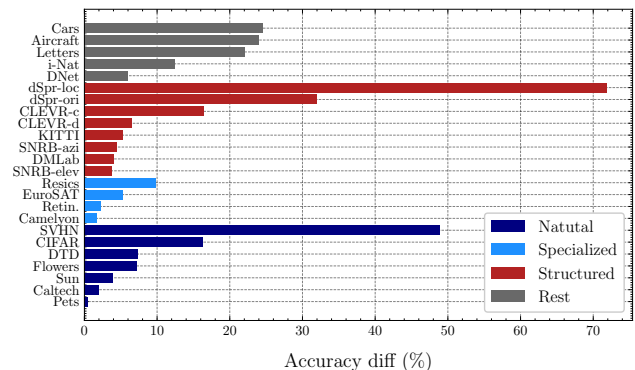


Figure 3. Bar plot of the accuracy differences between FSA-FiLM and NA for the offline case with 50 shots.

	CFR100	SVHN	dSp-loc	FGVC	Letters	DNet	iNat
EffNet-B0 (FSA-FiLM)	70.9	51.3	35.7	55.8	73.4	74.0	58.8
ConvNext (NA)	87.1	43.6	13.6	50.2	63.1	82.9	72.6
ConvNext-CosD	0.2	0.6	0.6	0.3	0.4	0.3	0.1

Table 5. Accuracy comparison between a pre-trained ConvNext on ImageNet-22k without body adaptation (NA) and a pre-trained EfficientNet-B0 on ImageNet-1k which is adapted on the first session (FSA-FiLM). We use the few-shot CIL setting (Sec. 4.3) and we report the accuracy (%) (\uparrow) after the last session. Results are averaged over 5 runs (mean \pm std). We also include the minimum cosine distance using the pre-trained ConvNext as in Figure 2.

To stress the importance of adaptation on datasets far from ImageNet, we compare FSA-FiLM with an EfficientNet-B0 backbone to the no-adaptation method with a ConvNext [27] pre-trained on Imagenet-22k. The total number of parameters for FSA-FiLM (backbone and FiLM parameters) is \sim 4M while for ConvNext is 348M. Table 5

shows that a small adapted backbone can significantly surpass the accuracy of a much larger pre-trained backbone for datasets far from ImageNet. We also compute the cosine distance measure for ConvNext and find that it is predictive of the performance of the unadapted ConvNext model and the benefits of adaptation. We show this in Table 5; note that for CIFAR100 the ConvNext’s cosine distance values are small relative to the other datasets (indicating that CIFAR100 is close to the pretraining distribution) whereas for EfficientNet the values in Figure 2 indicate that CIFAR100 is more out-of-distribution.

The main takeaway from these results is that when there is a large cosine distance (e.g. SVHN, dSprites, FGVC, Letters) FiLM adaptation of a light-weight backbone performs well – better even than applying LDA head adaptation to a much larger backbone trained on a much larger dataset. As the community employs ever-larger models and datasets, these results indicate that adapters are likely to continue to bring improvements over simply learning a classifier head (the NA baseline).

5. Discussion

We have presented FSA (-FiLM), a simple yet effective replay-free baseline for CIL which adapts a pre-trained backbone via full body adaptation or FiLM layers only at the first session of continual learning and then utilizes a flexible incrementally updated LDA classifier on top of the body. Extensive experiments in several CIL scenarios have shown that FSA outperforms previous SOTA baselines in most cases, thus, questioning the efficacy of current approaches to continuous body adaption. Furthermore, the experiments have revealed that FiLM layers are helpful when the amount of data available in the target domain is relatively low and the number of parameters in the neural network and the size of the source domain data set is large. For very large foundation models trained on very large source domain data sets, it is likely we are often in this situation and FiLM-like layers will be more effective than full-body adaptation, even when the target domain has a fairly large amount of data.

Limitations and future work. The main limitation of this work is inextricably linked with the distributional assumptions of CIL in general. If the data distribution at each session shifts considerably (e.g. the first session includes natural images while the next session includes images of numbers) then first session body adaptation is not suitable. In future work, we plan to combine FSA (-FiLM) with a memory method like GDumb to get the best of both worlds and deal with more challenging CIL scenarios.

Acknowledgements

We are grateful to John Bronskill for his guidance on how to use the HPC cluster. We also thank John Bronskill, Aliaksandra Shysheya, and Massimiliano Patacchiola for useful discussions. The experiments were carried out using resources provided by the Cambridge Tier-2 system operated by the University of Cambridge Research Computing Service <https://www.hpc.cam.ac.uk>. This work was funded by Toyota Motor Europe.

References

- [1] Hongjoon Ahn, Jihwan Kwak, Subin Lim, Hyeonsu Bang, Hyojun Kim, and Taesup Moon. Ss-il: Separated softmax for incremental learning. In *Proceedings of the IEEE/CVF International Conference on Computer Vision (ICCV)*, pages 844–853, October 2021. 2
- [2] Peyman Bateni, Raghav Goyal, Vaden Masrani, Frank Wood, and Leonid Sigal. Improved few-shot visual classification. In *Proceedings of the IEEE/CVF Conference on Computer Vision and Pattern Recognition*, pages 14493–14502, 2020. 2, 5
- [3] Charles Beattie, Joel Z Leibo, Denis Teplyashin, Tom Ward, Marcus Wainwright, Heinrich Küttler, Andrew Lefrancq, Simon Green, Víctor Valdés, Amir Sadik, et al. Deepmind lab. *arXiv preprint arXiv:1612.03801*, 2016. 14
- [4] John Bronskill, Daniela Massiceti, Massimiliano Patacchiola, Katja Hofmann, Sebastian Nowozin, and Richard Turner. Memory efficient meta-learning with large images. *Advances in Neural Information Processing Systems*, 34:24327–24339, 2021. 5, 15
- [5] Lucas Caccia, Rahaf Aljundi, Nader Asadi, Tinne Tuytelaars, Joelle Pineau, and Eugene Belilovsky. New insights on reducing abrupt representation change in online continual learning. *arXiv preprint arXiv:2203.03798*, 2022. 2
- [6] Gong Cheng, Junwei Han, and Xiaoqiang Lu. Remote sensing image scene classification: Benchmark and state of the art. *Proceedings of the IEEE*, 105(10):1865–1883, 2017. 14
- [7] Mircea Cimpoi, Subhansu Maji, Iasonas Kokkinos, Sammy Mohamed, and Andrea Vedaldi. Describing textures in the wild. In *Proceedings of the IEEE Conference on Computer Vision and Pattern Recognition*, pages 3606–3613, 2014. 14
- [8] MohammadReza Davari, Nader Asadi, Sudhir Mudur, Rahaf Aljundi, and Eugene Belilovsky. Probing representation forgetting in supervised and unsupervised continual learning. In *Proceedings of the IEEE/CVF Conference on Computer Vision and Pattern Recognition*, pages 16712–16721, 2022. 2
- [9] T. E. de Campos, B. R. Babu, and M. Varma. Character recognition in natural images. In *Proceedings of the International Conference on Computer Vision Theory and Applications, Lisbon, Portugal*, February 2009. 5, 14
- [10] Matthias De Lange, Rahaf Aljundi, Marc Masana, Sarah Parisot, Xu Jia, Aleš Leonardis, Gregory Slabaugh, and Tinne Tuytelaars. A continual learning survey: Defying forgetting in classification tasks. *IEEE Transactions on Pattern*

- Analysis and Machine Intelligence*, 44(7):3366–3385, 2021. 2
- [11] Li Fei-Fei, Robert Fergus, and Pietro Perona. One-shot learning of object categories. *IEEE Transactions on Pattern Analysis and Machine Intelligence*, 28(4):594–611, 2006. 14
- [12] Andreas Geiger, Philip Lenz, Christoph Stiller, and Raquel Urtasun. Vision meets robotics: The kitti dataset. *The International Journal of Robotics Research*, 32(11):1231–1237, 2013. 14
- [13] Tyler L Hayes and Christopher Kanan. Lifelong machine learning with deep streaming linear discriminant analysis. In *Proceedings of the IEEE/CVF conference on Computer Vision and Pattern Recognition workshops*, pages 220–221, 2020. 3
- [14] Kaiming He, Xiangyu Zhang, Shaoqing Ren, and Jian Sun. Deep residual learning for image recognition. In *Proceedings of the IEEE/CVF Conference on Computer Vision and Pattern Recognition*, pages 770–778, 2016. 5
- [15] Patrick Helber, Benjamin Bischke, Andreas Dengel, and Damian Borth. Eurosat: A novel dataset and deep learning benchmark for land use and land cover classification. *IEEE Journal of Selected Topics in Applied Earth Observations and Remote Sensing*, 12(7):2217–2226, 2019. 14
- [16] Michael Hersche, Geethan Karunaratne, Giovanni Cherubini, Luca Benini, Abu Sebastian, and Abbas Rahimi. Constrained few-shot class-incremental learning. In *Proceedings of the IEEE/CVF Conference on Computer Vision and Pattern Recognition*, pages 9057–9067, 2022. 2, 3
- [17] Elad Hoffer and Nir Ailon. Deep metric learning using triplet network. In *Similarity-Based Pattern Recognition: Third International Workshop, SIMBAD 2015, Copenhagen, Denmark, October 12-14, 2015. Proceedings 3*, pages 84–92. Springer, 2015. 14
- [18] Timothy Hospedales, Antreas Antoniou, Paul Micaelli, and Amos Storkey. Meta-learning in neural networks: A survey. *IEEE Transactions on Pattern Analysis and Machine Intelligence*, 44(9):5149–5169, 2021. 3
- [19] Justin Johnson, Bharath Hariharan, Laurens Van Der Maaten, Li Fei-Fei, C Lawrence Zitnick, and Ross Girshick. Clevr: A diagnostic dataset for compositional language and elementary visual reasoning. In *Proceedings of the IEEE/CVF Conference on Computer Vision and Pattern Recognition*, pages 2901–2910, 2017. 14
- [20] Kaggle and EyePacs. Kaggle diabetic retinopathy detection. <https://www.kaggle.com/c/diabetic-retinopathy-detection/data>, 2015. 14
- [21] Minsoo Kang, Jaeyoo Park, and Bohyung Han. Class-incremental learning by knowledge distillation with adaptive feature consolidation. In *Proceedings of the IEEE/CVF Conference on Computer Vision and Pattern Recognition*, pages 16071–16080, 2022. 2, 3
- [22] Diederik P Kingma and Jimmy Ba. Adam: A method for stochastic optimization. *arXiv preprint arXiv:1412.6980*, 2014. 13
- [23] Jonathan Krause, Michael Stark, Jia Deng, and Li Fei-Fei. 3d object representations for fine-grained categorization. In *Proceedings of the IEEE International Conference on Computer Vision Workshops*, pages 554–561, 2013. 5, 14
- [24] Alex Krizhevsky, Geoffrey Hinton, et al. Learning multiple layers of features from tiny images. 2009. 14
- [25] Yann LeCun, Fu Jie Huang, and Leon Bottou. Learning methods for generic object recognition with invariance to pose and lighting. In *Proceedings of the IEEE Conference on Computer Vision and Pattern Recognition*, volume 2, pages II–104. IEEE, 2004. 14
- [26] Timothée Lesort, Oleksiy Ostapenko, Diganta Misra, Md Rifat Arefin, Pau Rodríguez, Laurent Charlin, and Irina Rish. Scaling the number of tasks in continual learning. *arXiv preprint arXiv:2207.04543*, 2022. 2
- [27] Zhuang Liu, Hanzi Mao, Chao-Yuan Wu, Christoph Feichtenhofer, Trevor Darrell, and Saining Xie. A convnet for the 2020s. In *Proceedings of the IEEE/CVF Conference on Computer Vision and Pattern Recognition*, pages 11976–11986, 2022. 8
- [28] Vincenzo Lomonaco and Davide Maltoni. Core50: A new dataset and benchmark for continuous object recognition. In *Conference on Robot Learning*, pages 17–26. PMLR, 2017. 5, 14
- [29] Zheda Mai, Ruiwen Li, Jihwan Jeong, David Quispe, Hyunwoo Kim, and Scott Sanner. Online continual learning in image classification: An empirical survey. *Neurocomputing*, 469:28–51, 2022. 3
- [30] Subhransu Maji, Esa Rahtu, Juho Kannala, Matthew Blaschko, and Andrea Vedaldi. Fine-grained visual classification of aircraft. *arXiv preprint arXiv:1306.5151*, 2013. 5, 14
- [31] Loic Matthey, Irina Higgins, Demis Hassabis, and Alexander Lerchner. dsprites: Disentanglement testing sprites dataset. <https://github.com/deepmind/dsprites-dataset/>, 2017. 14
- [32] Thomas Mensink, Jakob Verbeek, Florent Perronnin, and Gabriela Csurka. Distance-based image classification: Generalizing to new classes at near-zero cost. *IEEE Transactions on Pattern Analysis and Machine Intelligence*, 35(11):2624–2637, 2013. 2
- [33] Yuval Netzer, Tao Wang, Adam Coates, Alessandro Bischoff, Bo Wu, and Andrew Y Ng. Reading digits in natural images with unsupervised feature learning. 2011. 14
- [34] Maria-Elena Nilsback and Andrew Zisserman. Automated flower classification over a large number of classes. In *2008 Sixth Indian Conference on Computer Vision, Graphics & Image Processing*, pages 722–729. IEEE, 2008. 14
- [35] Oleksiy Ostapenko, Timothee Lesort, Pau Rodríguez, Md Rifat Arefin, Arthur Douillard, Irina Rish, and Laurent Charlin. Continual learning with foundation models: An empirical study of latent replay. In *Conference on Lifelong Learning Agents*, pages 60–91. PMLR, 2022. 2, 3
- [36] Omkar M Parkhi, Andrea Vedaldi, Andrew Zisserman, and CV Jawahar. Cats and dogs. In *2012 IEEE Conference on Computer Vision and Pattern Recognition*, pages 3498–3505. IEEE, 2012. 14
- [37] Adam Paszke, Sam Gross, Francisco Massa, Adam Lerer, James Bradbury, Gregory Chanan, Trevor Killeen, Zeming

- Lin, Natalia Gimelshein, Luca Antiga, et al. Pytorch: An imperative style, high-performance deep learning library. *Advances in Neural Information Processing Systems*, 32, 2019. [5](#)
- [38] Can Peng, Kun Zhao, Tianren Wang, Meng Li, and Brian C Lovell. Few-shot class-incremental learning from an open-set perspective. In *Computer Vision–ECCV 2022: 17th European Conference, Tel Aviv, Israel, October 23–27, 2022, Proceedings, Part XXV*, pages 382–397. Springer, 2022. [2](#), [6](#), [7](#), [8](#), [14](#), [28](#), [29](#)
- [39] Xingchao Peng, Qinxun Bai, Xide Xia, Zijun Huang, Kate Saenko, and Bo Wang. Moment matching for multi-source domain adaptation. In *Proceedings of the IEEE/CVF Conference on Computer Vision and Pattern Recognition*, pages 1406–1415, 2019. [5](#), [14](#)
- [40] Ethan Perez, Florian Strub, Harm De Vries, Vincent Dumoulin, and Aaron Courville. FiLM: Visual reasoning with a general conditioning layer. In *Proceedings of the AAAI Conference on Artificial Intelligence*, volume 32, 2018. [2](#), [3](#)
- [41] Ameya Prabhu, Philip HS Torr, and Puneet K Dokania. GDumb: A simple approach that questions our progress in continual learning. In *European Conference on Computer Vision*, pages 524–540. Springer, 2020. [2](#), [5](#), [6](#), [13](#), [14](#)
- [42] Sylvestre-Alvise Rebuffi, Alexander Kolesnikov, Georg Sperl, and Christoph H Lampert. icarl: Incremental classifier and representation learning. In *Proceedings of the IEEE/CVF Conference on Computer Vision and Pattern Recognition*, pages 2001–2010, 2017. [2](#)
- [43] James Requeima, Jonathan Gordon, John Bronskill, Sebastian Nowozin, and Richard E Turner. Fast and flexible multi-task classification using conditional neural adaptive processes. *Advances in Neural Information Processing Systems*, 32, 2019. [3](#), [5](#)
- [44] Aliaksandra Shysheya, John Bronskill, Massimiliano Patacchiola, Sebastian Nowozin, and Richard E Turner. Fit: Parameter efficient few-shot transfer learning for personalized and federated image classification. *arXiv preprint arXiv:2206.08671*, 2022. [3](#), [5](#)
- [45] Mingxing Tan and Quoc Le. Efficientnet: Rethinking model scaling for convolutional neural networks. In *International Conference on Machine Learning*, pages 6105–6114. PMLR, 2019. [5](#)
- [46] Xiaoyu Tao, Xiaopeng Hong, Xinyuan Chang, Songlin Dong, Xing Wei, and Yihong Gong. Few-shot class-incremental learning. In *Proceedings of the IEEE/CVF Conference on Computer Vision and Pattern Recognition*, pages 12183–12192, 2020. [5](#)
- [47] Grant Van Horn, Oisin Mac Aodha, Yang Song, Yin Cui, Chen Sun, Alex Shepard, Hartwig Adam, Pietro Perona, and Serge Belongie. The iNaturalist Species Classification and Detection Dataset. In *Proceedings of the IEEE Conference/CVF on Computer Vision and Pattern Recognition*, pages 8769–8778, 2018. [5](#), [14](#)
- [48] Bastiaan S Veeling, Jasper Linmans, Jim Winkens, Taco Cohen, and Max Welling. Rotation equivariant cnns for digital pathology. In *International Conference on Medical image computing and computer-assisted intervention*, pages 210–218. Springer, 2018. [14](#)
- [49] Oriol Vinyals, Charles Blundell, Timothy Lillicrap, Daan Wierstra, et al. Matching networks for one shot learning. *Advances in Neural Information Processing Systems*, 29, 2016. [5](#), [8](#)
- [50] C. Wah, S. Branson, P. Welinder, P. Perona, and S. Belongie. Technical Report CNS-TR-2011-001, California Institute of Technology, 2011. [5](#), [14](#)
- [51] Yaqing Wang, Quanming Yao, James T Kwok, and Lionel M Ni. Generalizing from a few examples: A survey on few-shot learning. *ACM computing surveys (csur)*, 53(3):1–34, 2020. [3](#)
- [52] Zifeng Wang, Zizhao Zhang, Sayna Ebrahimi, Ruoxi Sun, Han Zhang, Chen-Yu Lee, Xiaoqi Ren, Guolong Su, Vincent Perot, Jennifer Dy, et al. Dualprompt: Complementary prompting for rehearsal-free continual learning. In *Computer Vision–ECCV 2022: 17th European Conference, Tel Aviv, Israel, October 23–27, 2022, Proceedings, Part XXVI*, pages 631–648. Springer, 2022. [2](#)
- [53] Zifeng Wang, Zizhao Zhang, Chen-Yu Lee, Han Zhang, Ruoxi Sun, Xiaoqi Ren, Guolong Su, Vincent Perot, Jennifer Dy, and Tomas Pfister. Learning to prompt for continual learning. In *Proceedings of the IEEE/CVF Conference on Computer Vision and Pattern Recognition*, pages 139–149, 2022. [2](#)
- [54] Guile Wu, Shaogang Gong, and Pan Li. Striking a balance between stability and plasticity for class-incremental learning. In *Proceedings of the IEEE/CVF International Conference on Computer Vision (ICCV)*, pages 1124–1133, 2021. [2](#)
- [55] Tz-Ying Wu, Gurumurthy Swaminathan, Zhizhong Li, Avinash Ravichandran, Nuno Vasconcelos, Rahul Bhotika, and Stefano Soatto. Class-incremental learning with strong pre-trained models. In *Proceedings of the IEEE/CVF Conference on Computer Vision and Pattern Recognition*, pages 9601–9610, 2022. [5](#)
- [56] Yue Wu, Yinpeng Chen, Lijuan Wang, Yuancheng Ye, Zicheng Liu, Yandong Guo, and Yun Fu. Large scale incremental learning. In *Proceedings of the IEEE/CVF International Conference on Computer Vision (ICCV)*, pages 374–382, 2019. [2](#)
- [57] Jianxiong Xiao, James Hays, Krista A Ehinger, Aude Oliva, and Antonio Torralba. Sun database: Large-scale scene recognition from abbey to zoo. In *2010 IEEE Conference on Computer Vision and Pattern Recognition*, pages 3485–3492. IEEE, 2010. [14](#)
- [58] Shipeng Yan, Jiangwei Xie, and Xuming He. Der: Dynamically expandable representation for class incremental learning. In *Proceedings of the IEEE/CVF Conference on Computer Vision and Pattern Recognition*, pages 3014–3023, 2021. [2](#)
- [59] Jason Yosinski, Jeff Clune, Yoshua Bengio, and Hod Lipson. How transferable are features in deep neural networks? *Advances in Neural Information Processing Systems*, 27, 2014. [3](#)
- [60] Lu Yu, Bartłomiej Twardowski, Xialei Liu, Luis Herranz, Kai Wang, Yongmei Cheng, Shangling Jui, and Joost van de Weijer. Semantic drift compensation for class-incremental

- learning. In *Proceedings of the IEEE/CVF conference on computer vision and pattern recognition*, pages 6982–6991, 2020. 5, 6, 14
- [61] Xiaohua Zhai, Joan Puigcerver, Alexander Kolesnikov, Pierre Ruysen, Carlos Riquelme, Mario Lucic, Josip Djolonga, Andre Susano Pinto, Maxim Neumann, Alexey Dosovitskiy, et al. A large-scale study of representation learning with the visual task adaptation benchmark. *arXiv preprint arXiv:1910.04867*, 2019. 5, 13
- [62] Chi Zhang, Nan Song, Guosheng Lin, Yun Zheng, Pan Pan, and Yinghui Xu. Few-shot incremental learning with continually evolved classifiers. In *Proceedings of the IEEE/CVF Conference on Computer Vision and Pattern Recognition*, pages 12455–12464, 2021. 5, 7
- [63] Bowen Zhao, Xi Xiao, Guojun Gan, Bin Zhang, and Shu-Tao Xia. Maintaining discrimination and fairness in class incremental learning. In *Proceedings of the IEEE/CVF Conference on Computer Vision and Pattern Recognition*, pages 13208–13217, 2020. 2
- [64] Da-Wei Zhou, Fu-Yun Wang, Han-Jia Ye, Liang Ma, Shiliang Pu, and De-Chuan Zhan. Forward compatible few-shot class-incremental learning. In *Proceedings of the IEEE/CVF Conference on Computer Vision and Pattern Recognition*, pages 9046–9056, 2022. 3, 5, 6, 7, 8, 13, 14, 28, 29

A. Datasets

The exact numbers of training samples and classes for each dataset used in the experiments of Section 4 in the main paper are given in Table 6. For datasets with more than 120k training instances in VTAB+, due to hardware limitations, we randomly sample 120k images and the associated labels and we consider this subset as the full training set. For instance, when we use dSprites-location dataset in a 50-shot setting, we first randomly sample 120k examples and then we randomly pick 50 images for each one of the 16 classes. For DomainNet and iNaturalist we apply a different procedure (see Appendix B for details).

For evaluation, we consider the protocol used in [61] on the 19 datasets in VTAB, where a balanced dataset of 2k images is created by randomly sampling images from the full test dataset. For FGVC-Aircraft, Cars, and Letters the full test dataset is utilized. We also use the full test dataset for evaluation in the high-shot Class-Incremental Learning (CIL) setting.

B. Dataset Information for the Class-Incremental Learning Experiments

In Table 7, we present detailed information about the Class-Incremental Learning Experiments (CIL) experiments that are in Section 4.3 in the main paper, such as the number of total sessions, number of train instances, and classes per session. Next, we discuss the exact setup for DomainNet and iNaturalist.

DomainNet & iNaturalist. DomainNet and iNaturalist are the only datasets for which we follow a different pre-processing procedure from the one described in Appendix A in order to create a few-shot CIL scenario similar to the ones considered in the literature. This is due to the large number of classes (iNaturalist has 10,000 classes) and different domains (DomainNet includes images from 6 domains) these datasets have.

DomainNet is a large-scale dataset of ~ 0.6 M images lying in 6 different domains (clipart, infograph, painting, quickdraw, real, sketch) and categorized into 365 distinct classes. These classes can be grouped into 24 superclasses: furniture, mammal, tool, cloth, electricity, building, office, human body, road transportation, food, nature, cold-blooded, music, fruit, sport, tree, bird, vegetable, shape, kitchen, Water transportation, sky transportation, insects, and others. In our CIL experiments, we use 60 classes from the superclasses with an adequate number of instances (> 150): furniture, mammal, tool, cloth, electricity, and road transportation. To the best of our knowledge, this is the first time such a dataset is considered for CIL problems. Table 8 summarizes the DomainNet classes we use for the CIL experiments. To build the 50-shot CIL setting of Sec-

tion 4.3, we randomly sample 50 images per class and the rest of the images are used for evaluation.

The iNaturalist is another large-scale dataset, comprising ~ 2.7 million images of 10,000 species. The species can be divided into 10 general categories: amphibians, animalia, arachnids, birds, fungi, insects, mammals, mollusks, plants, and reptiles. Due to the dataset’s large size, we have opted to use the “mini” version of the training dataset² which has 50 images per class, and thus, this is the only dataset from the few-shot CIL experiments that we do not repeat for 5 times since the (mini) train dataset is already in a 50-shot setting. For evaluation, we use the validation data with 10 images per class. The number of classes considered for the CIL experiments is reduced from 10,000 to 100; 10 classes per superclass (10 superclasses/sessions). Specific details are given in Tables 9 and 10.

C. Extra Training Details

Due to the large number of experiments and datasets we tried to keep the hyperparameter tuning to a minimum by choosing a set of hyperparameters that works fairly well across all datasets and settings. We have not used any data augmentation in our experiments and all images have been scaled to 224×224 pixels. The only exception is the experiments on CIFAR100, and CUB200 under the few-shot+ setting. There, for comparability reasons, we followed the exact experimental settings as in [64] where standard data augmentation techniques (e.g. random flips and crops) were utilized. Moreover, when we used ResNet-20 for CIFAR100 we maintained the original image size (32×32).

Computing Infrastructure Details & Code. All the experiments of Section 4 have been carried out on a Linux machine with a single NVIDIA-A100 (80GB memory) GPU. Our PyTorch-based code will be made available via a public repository after the review period.

Optimization Details. In all experiments, we train the models using a batch size of 256. Apart from GDumb, for the rest of the methods, EfficientNet-B0 backbones are optimized with the Adam optimizer [22] while for ResNet architectures we opt for SGD with momentum set to 0.9. For GDumb, we follow [41] and we use SGD with momentum. For FACT [64] and FSA with pre-trained EfficientNet-B0 backbone, we set the initial learning rate to 0.0001 with scheduled decays by a factor of 0.5 every 50 epochs while for FSA-FiLM, we set it to 0.005. We train all full-body adaptation methods for 200 epochs and the FSA-FiLM for 150 epochs (except for the high-shot setting where we

²We use the data from the 2021 competition, available at https://github.com/visipedia/inat_comp/tree/master/2021.

Datasets	# Classes	# Train instances	ALL	CIL
Caltech101 [11]	102	3,060	✓	✗
CIFAR100 [24]	100	50,000	✓	✓
Flowers102 [34]	102	1,020	✓	✗
Pets [36]	37	3,680	✓	✗
Sun397 [57]	397	76,127	✓	✗
SVHN [33]	10	73,257	✓	✓
DTD [7]	47	1,880	✓	✗
EuroSAT [15]	10	27,000	✓	✗
Resics45 [6]	45	31,500	✓	✗
Patch Camelyon [48]	2	262,144	✓	✗
Retinopathy [20]	5	35,126	✓	✗
CLEVR-count [19]	8	70,000	✓	✗
CLEVR-dist [19]	6	70,000	✓	✗
dSprites-loc [31]	16	737,280	✓	✓
dSprites-ori [31]	16	737,280	✓	✗
SmallNORB-azi [25]	18	24,300	✓	✗
SmallNORB-elev [25]	9	24,300	✓	✗
DMLab [3]	6	65,550	✓	✗
KITTI-dist [12]	4	6,347	✓	✗
FGVC-Aircraft [30]	100	6,667	✓	✓
Cars [23]	196	8,144	✓	✓
Letters [9]	62	74,107	✓	✓
DomainNet [39]	60 (345 [†])	569,010	✗	✓
iNaturalist [47]	100 (10,000 [†])	500,000	✗	✓
Core50 [28]	50	119,894	✓	✓
CUB200 [50]	200	11,788	✗	✓

Table 6. Information concerning all datasets used in the experiments. † denotes the number of classes of the original dataset before they are modified for the continual learning scenarios (see Appendix B for more details). The first 22 datasets form the VTAB+ collection. We also indicate whether a dataset has been used in the offline experiments in Section 4.2 of the main paper which use all the available training data (ALL). Similarly, we indicate which datasets are considered for the Class-Incremental Learning settings in Section 4.

use 200 epochs for fair time comparisons). For the few-shot+ CIL scenario, we follow the training setup of [64]. The weights of the pre-trained EfficientNet-B0 have been obtained from <https://github.com/lukemelas/EfficientNet-PyTorch> while for the pre-trained weights of ResNet-18 and ConvNext, we use the following repository <https://github.com/rwightman/pytorch-image-models>.

Competitors. We found empirically that the recommended hyperparameter values (learning rates, cutmix parameters, SGDR schedule) for GDumb in [41] work well in practice and we use these throughout the experiments. Similarly, for FACT, we use the default values $\alpha = 0.5, \gamma = 0.01, V =$ number of new classes in total [64]. For ALICE, following [38], the projection head is a two-layer MLP with a hidden feature size of 2048 and ReLU as the activation

function. All the other hyperparameters (scale factor s , margin m , etc.) are set as in [38]. For E-EWC+SDC, a triplet loss [17] is used as in [60] and the final embeddings of 640 dimensions are normalized.

D. Additional Results

In this section, we provide tables with the exact accuracies for each one of the datasets used in the experiments under different settings. We have run extra experiments on VTAB+ using meta-learned FiLM adapters in the offline setting and we report accuracies. Additionally, we perform a comparison between different backbones in the offline setting: EfficientNet-B0 and ResNet-18. For the high-shot setting, apart from the four datasets utilized in the main paper, we also deploy the methods on SVHN and present accuracies by session. Finally, accuracies at each session for all three CIL settings are provided.

CIL setting	Datasets	S	N_1	$ \mathcal{Y}_1 $	N_s	$ \mathcal{Y}_s $
High-shot	CIFAR100	10	5k	10	5k	10
	SVHN	5	$\sim 19k$	2	$\sim 14k$	2
	dSprites-loc	7	24k	4	12k	2
	FGVC-Aircraft	10	667	10	~ 670	10
	Cars	10	652	15	~ 830	20
	Letters	11	$\sim 11k$	12	$\sim 5k$	5
Few-shot+	CIFAR100	9	30k	60	25	5
	CUB200	11	3k	100	50	10
Few-shot	CIFAR100	9	1k	20	500	10
	SVHN	5	100	2	100	2
	dSprites-loc	7	200	4	100	2
	FGVC-Aircraft	9	1k	20	500	10
	Cars	9	1484	36	~ 830	20
	Letters	11	600	12	250	5
	DomainNet	9	600	12	300	6
	iNaturalist	9	1k	20	500	10

Table 7. Detailed CIL settings for the experiments of Section 4.3. We report the total number of sessions (S), the number of train instances (N_1), and the number of classes ($|\mathcal{Y}_1|$) of the first session and the rest of the sessions ($N_s, |\mathcal{Y}_s|, s > 1$).

Head Comparison. Here we provide the exact accuracies for each dataset based on Section 4.2 and Figure 1 of the main paper. Tables 11, 12, 13, and 14 give the offline accuracies for the no adaptation (NA) method for 5, 10, 50 shots, and all training data, respectively. Similar information for the FiLM adaptation method (A-FiLM) is given in Tables 15, 16, 17, and 18. Finally, Tables 19, 20, 21, and 22 provide the corresponding accuracies for the full-body adaptation method (A-FB).

Meta-learned FiLM Adapters. We consider experiments in the offline setting with meta-learned FiLM adapters. We use the meta-trained FiLM adapters as presented in [4]. The results for meta-learned FiLM adapters, as well as for no-adaptation (NA), FiLM (fine-tuned) adaptation (FiLM), and full body adaptation methods, are summarized in Tables 26, 27, and 28, for 5, 10, and 50 shots, respectively. We observe that the meta-trained FiLM adapters work better than NA in all cases, but they fail to compete with the fine-tuned FiLM adapters. Notice that as the number of shots increases, the accuracy difference between meta-learned and fine-tuned FiLM adapters also increases.

FiLM Adaptation: EfficientNet-B0 vs ResNet-18. To assess how different backbone architectures affect the performance of the no-adaptation and FiLM adaptation method, we compare ResNet-18 and EfficientNet-B0 (EN) backbones in Tables 23, 24, and 25, for 5, 10, and 50 shots, respectively. All tables demonstrate the superiority of

EfficientNet-B0, regardless of the adaptation method. The tables also show that, regardless of backbone architecture and number of shots, FiLM adaptation provides significant performance benefits.

High-shot CIL: Accuracies per Session. We provide detailed accuracies for each incremental session for all baselines in the high-shot CIL setting. The accuracies for CIFAR100, CORE50, SVHN, dSprites-loc, FGVC-Aircraft, Cars, and Letters can be found in Tables 29, 30, 31, 32, 33, 34, and 35, respectively. For GDumb, we provide results with a memory buffer of size 1k and 5k.

Few-shot+ CIL: Accuracies per Session. We provide detailed accuracy for each incremental session for all baselines in the few-shot+ CIL setting. The accuracies for CIFAR100 and CUB200 can be found in Tables 36 and 37, respectively.

Few-shot CIL: Accuracies per Session. We provide detailed accuracy (+ error bars) for each incremental session for all baselines in the few-shot CIL setting. The accuracies for CIFAR100, SVHN, dSprites-location, FGVC-Aircraft, Letters, DomainNet, and iNaturalist can be found in Tables 38, 39, 40, 41, 42, 43, and 44, respectively.

FSA-FiLM vs GDumb The trade-off between accuracy and training time for different continual learning methods on CIFAR100 and CORE50 is illustrated in Fig. 4. Several different memory sizes are used for GDumb. FSA-FiLM attains the highest accuracy (and the lowest PPDR) $\approx 13.5x$ faster than GDumb with a 5k memory buffer on CIFAR100 while on CORE50, GDumb requires at least a 5K memory buffer to outperform FSA-FiLM and $\approx 3x$ more training time than FSA-FiLM. Notice that FACT is unable to perform well under this setting due to the small number of available classes in the first session.

Domain	Clipart	Infograph	Painting	Quickdraw	Real	Sketch
Superclass	Furniture	Mammal	Tool	Cloth	Electricity	Road Transportation
Classes	Clipart	Infograph	Painting	Quickdraw	Real	Sketch
	Furniture	Mammal	Tool	Cloth	Electricity	Road Transportation
	Couch (1)	Cat (11)	Anvil (21)	Belt (31)	Calculator (41)	Ambulance (51)
	Fence (2)	Dolphin (12)	Basket (22)	Camouflage (32)	Computer (42)	Bus (52)
	Streetlight (3)	Squirrel (13)	Rifle (23)	Eyeglasses (33)	Fan (43)	Motorbike (53)
	Table (4)	Zebra (14)	Axe (24)	Helmet (34)	Oven (44)	Train (54)
	Toothbrush (5)	Cow (15)	Dumbbell (25)	Necklace (35)	Dishwasher (45)	Bicycle (55)
	Vase (6)	Elephant (16)	Pliers (26)	Rollerskates (36)	Headphones (46)	Car (56)
	Bed (7)	Pig (17)	Saw (27)	Sock (37)	Microwave (47)	Truck (57)
	Fireplace (8)	Tiger (18)	Skateboard (28)	Underwear (38)	Radio (48)	Bulldozer (58)
Teapot (9)	Dog (19)	Bandage (29)	Bowtie (39)	Stereo (49)	Firetruck (59)	
Lantern (10)	Rabbit (20)	Paint Can (30)	Crown (40)	Toaster (50)	Tractor (60)	

Table 8. DomainNet classes (class id in parentheses) used for the few-shot CIL setting.

Session	Superclass				
	Amphibians 1	Animalia 2	Arachnids 3	Birds 4	Fungi 5
Classes	Ascaphus truei	Lumbricus terrestris	Eratigena duellica	Accipiter badius	Herpothallon rubrocinctum
	Bombina orientalis	Sabella spallanzanii	Atypoides riversi	Accipiter cooperii	Chrysothrix candelaris
	Bombina variegata	Serpula columbiana	Aculepeira ceropegia	Accipiter gentilis	Apiosporina morbosa
	Anaxyrus americanus	Spirobranchus cariniferus	Agalenatea redii	Accipiter nisus	Acarospora socialis
	Anaxyrus boreas	Hemisclopendra marginata	Araneus bicentarius	Accipiter striatus	Physcia adscendens
	Anaxyrus cognatus	Scolopendra cingulata	Araneus diadematus	Accipiter trivirgatus	Physcia aipolia
	Anaxyrus fowleri	Scolopendra heros	Araneus marmoreus	Aegypius monachus	Physcia millegrana
	Anaxyrus punctatus	Scolopendra polymorpha	Araneus quadratus	Aquila audax	Physcia stellaris
	Anaxyrus quercicus	Scutigera coleoptrata	Araneus trifolium	Aquila chrysaetos	Candelaria concolor
	Anaxyrus speciosus	Ommatolius moreleti	Araniella displicata	Aquila heliaca	Cladonia chlorophaea

Table 9. Classes used from iNaturalist to create the few-shot CIL setting. (table continues to Table 10).

Session	Superclass				
	Insects 6	Mammals 7	Mollusks 8	Plants 9	Reptiles 10
Classes	Aptera fusca	Antilocapra americana	Ensis leei	Bryum argenteum	Alligator mississippiensis
	Panchlora nivea	Balaenoptera acutorostrata	Clinocardium nuttallii	Rhodobryum ontariense	Caiman crocodilus
	Pycnoscelus surinamensis	Megaptera novaeangliae	Dinocardium robustum	Leucolepis acanthoneura	Crocodylus acutus
	Blatta orientalis	Aepyceros melampus	Tridacna maxima	Plagiommium cuspidatum	Crocodylus moreletii
	Periplaneta americana	Alcelaphus buselaphus	Donax gouldii	Plagiommium insigne	Crocodylus niloticus
	Periplaneta australasiae	Antilocas marsupialis	Donax variabilis	Rhizomnium glabrescens	Crocodylus porosus
	Periplaneta fuliginosa	Bison bison	Dreissena polymorpha	Dicranum scoparium	Sphenodon punctatus
	Pseudomops septentrionalis	Bos taurus	Mya arenaria	Ceratodon purpureus	Acanthoecerus atricollis
	Arrhenodes minutus	Boselaphus tragocamelus	Cyrtopleura costata	Leucobryum glaucum	Agama atra
	Agrilus planipennis	Bubalus bubalis	Geukensia demissa	Funaria hygrometrica	Agama picticauda

Table 10. Classes used from iNaturalist to create the few-shot CIL setting. The first part can be found in Table 9.

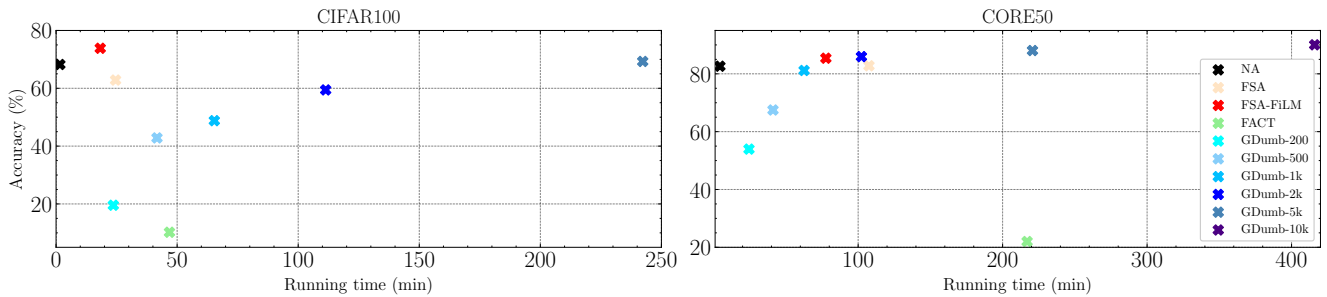


Figure 4. Last session’s test accuracy (\uparrow) and run time (\downarrow) for the “high-shot CIL” setting of Sec. 4.3. GDumb- m refers to memory buffer sizes $m \in \{200, 500, 1k, 2k, 5k, 10k^*\}$. We use a memory buffer of 10k images only for CORE50.

Dataset	NCM	LDA	Linear
Caltech101	85.7 \pm 0.9	88.2 \pm 0.8	87.2 \pm 0.7
CIFAR100	40.2 \pm 1.5	42.7 \pm 1.6	42.3 \pm 1.3
Flowers102	71.5 \pm 0.6	76.1 \pm 0.4	75.7 \pm 0.8
Pets	83.0 \pm 1.5	82.4 \pm 1.6	82.5 \pm 1.5
Sun397	41.0 \pm 0.9	41.9 \pm 1.0	42.9 \pm 0.7
SVHN	13.5 \pm 1.6	16.5 \pm 1.1	15.0 \pm 1.4
DTD	48.2 \pm 1.0	48.9 \pm 1.7	49.2 \pm 1.8
EuroSAT	72.1 \pm 1.9	76.3 \pm 1.8	74.6 \pm 2.0
Resiscs45	55.2 \pm 1.2	58.8 \pm 1.4	58.9 \pm 1.2
Patch Camelyon	59.6 \pm 8.7	59.8 \pm 7.2	59.0 \pm 6.4
Retinopathy	26.3 \pm 2.5	25.6 \pm 1.6	24.3 \pm 1.7
CLEVR-count	22.2 \pm 0.8	23.1 \pm 1.1	22.6 \pm 0.7
CLEVR-dist	23.0 \pm 2.7	24.5 \pm 2.3	24.4 \pm 2.2
dSprites-loc	7.5 \pm 0.7	8.5 \pm 0.6	7.3 \pm 0.6
dSprites-ori	13.1 \pm 1.2	16.2 \pm 0.8	14.8 \pm 1.1
SmallNORB-azi	6.8 \pm 0.6	9.3 \pm 0.8	8.8 \pm 1.0
SmallNORB-elev	13.0 \pm 1.5	15.1 \pm 0.6	14.5 \pm 0.9
DMLab	22.2 \pm 0.8	22.1 \pm 1.3	23.8 \pm 0.8
KITTI-dist	50.0 \pm 1.3	51.4 \pm 2.7	51.9 \pm 3.1
FGVC-Aircraft	19.4 \pm 0.6	22.1 \pm 1.0	22.7 \pm 0.6
Cars	20.0 \pm 0.6	22.6 \pm 0.6	22.0 \pm 0.7
Letters	28.3 \pm 1.8	36.1 \pm 2.1	34.0 \pm 1.3
Average acc	37.4	39.5	39.0

Table 11. Accuracy comparison between NCM, LDA, and Linear head without using any adaptation (NA method). The reported results are based on **5** shots and averaged over 5 runs (mean \pm std). A pre-trained EfficientNet-B0 is used as a backbone in all cases.

Dataset	NCM	LDA	Linear
Caltech101	88.5 \pm 0.9	90.0 \pm 0.8	89.6 \pm 0.7
CIFAR100	45.8 \pm 1.0	50.1 \pm 1.5	49.2 \pm 1.1
Flowers102	77.2 \pm 0.2	83.9 \pm 0.3	81.9 \pm 0.2
Pets	85.8 \pm 1.0	86.4 \pm 0.7	86.1 \pm 0.5
Sun397	47.1 \pm 1.3	49.0 \pm 1.3	49.7 \pm 0.8
SVHN	15.5 \pm 2.3	19.4 \pm 2.9	18.1 \pm 2.6
DTD	53.8 \pm 0.3	55.6 \pm 0.6	56.3 \pm 0.7
EuroSAT	76.6 \pm 1.2	82.1 \pm 0.9	80.2 \pm 0.9
Resiscs45	60.7 \pm 1.3	65.5 \pm 1.1	65.9 \pm 1.2
Patch Camelyon	63.0 \pm 5.3	66.5 \pm 3.7	65.3 \pm 4.7
Retinopathy	27.5 \pm 3.2	27.1 \pm 2.2	26.1 \pm 1.8
CLEVR-count	24.0 \pm 0.4	25.7 \pm 0.6	24.9 \pm 0.6
CLEVR-dist	24.2 \pm 1.2	26.3 \pm 1.1	26.3 \pm 1.4
dSprites-loc	7.5 \pm 0.5	8.7 \pm 0.3	7.9 \pm 0.3
dSprites-ori	14.2 \pm 0.9	18.2 \pm 0.7	16.4 \pm 1.0
SmallNORB-azi	8.4 \pm 0.4	9.5 \pm 1.1	9.5 \pm 0.7
SmallNORB-elev	13.6 \pm 0.8	16.5 \pm 1.1	16.2 \pm 0.7
DMLab	25.1 \pm 1.1	25.7 \pm 1.2	27.2 \pm 1.3
KITTI-dist	50.1 \pm 0.8	52.9 \pm 1.5	52.0 \pm 1.8
FGVC-Aircraft	23.1 \pm 0.4	28.5 \pm 0.4	27.0 \pm 0.4
Cars	25.4 \pm 0.5	30.4 \pm 0.5	30.7 \pm 0.4
Letters	34.2 \pm 0.8	45.6 \pm 0.8	45.2 \pm 1.4
Average acc	40.5	43.8	43.3

Table 12. Accuracy comparison between NCM, LDA, and Linear head without using any adaptation (NA method). The reported results are based on **10** shots and averaged over 5 runs (mean \pm std). A pre-trained EfficientNet-B0 is used as a backbone in all cases.

Dataset	NCM	LDA	Linear
Caltech101	90.4 \pm 0.6	91.9 \pm 0.5	93.0 \pm 0.4
CIFAR100	52.0 \pm 0.9	57.4 \pm 1.0	60.9 \pm 1.0
Flowers102	77.2 \pm 0.2	83.9 \pm 0.3	81.9 \pm 0.2
Pets	88.2 \pm 0.3	89.5 \pm 0.4	89.9 \pm 0.6
Sun397	52.6 \pm 1.1	55.9 \pm 1.0	58.4 \pm 0.8
SVHN	19.3 \pm 1.7	28.3 \pm 1.1	28.9 \pm 1.1
DTD	58.5 \pm 0.0	61.1 \pm 0.0	65.4 \pm 0.2
EuroSAT	81.7 \pm 0.6	87.7 \pm 0.9	88.2 \pm 0.7
Resiscs45	66.6 \pm 0.7	73.5 \pm 0.9	78.2 \pm 0.7
Patch Camelyon	70.9 \pm 5.4	76.2 \pm 1.1	76.2 \pm 1.5
Retinopathy	29.2 \pm 2.2	32.9 \pm 2.2	32.9 \pm 1.9
CLEVR-count	26.3 \pm 1.5	30.1 \pm 1.0	31.2 \pm 1.0
CLEVR-dist	27.8 \pm 0.8	32.2 \pm 1.1	31.7 \pm 1.0
dSprites-loc	9.3 \pm 0.8	11.9 \pm 0.4	9.9 \pm 0.6
dSprites-ori	14.9 \pm 0.5	20.1 \pm 1.1	18.7 \pm 2.2
SmallNORB-azi	9.5 \pm 0.6	12.3 \pm 0.8	12.1 \pm 1.1
SmallNORB-elev	15.2 \pm 1.3	19.1 \pm 0.7	20.0 \pm 0.5
DMLab	29.1 \pm 0.3	30.6 \pm 0.3	32.3 \pm 0.7
KITTI-dist	53.2 \pm 0.9	61.4 \pm 2.3	60.7 \pm 3.2
FGVC-Aircraft	30.9 \pm 0.5	41.0 \pm 0.7	46.1 \pm 0.6
Cars	33.7 \pm 0.0	43.3 \pm 0.0	46.5 \pm 0.2
Letters	43.1 \pm 1.0	57.6 \pm 0.8	65.9 \pm 1.1
Average acc	44.5	49.9	51.3

Table 13. Accuracy comparison between NCM, LDA, and Linear head without using any adaptation (NA method). The reported results are based on **50** shots and averaged over 5 runs (mean \pm std). A pre-trained EfficientNet-B0 is used as a backbone in all cases.

Dataset	NCM	LDA	Linear
Caltech101	90.4 \pm 0.6	91.9 \pm 0.5	93.0 \pm 0.4
CIFAR100	53.5 \pm 1.6	68.2 \pm 1.7	68.3 \pm 0.8
Flowers102	77.2 \pm 0.2	83.9 \pm 0.3	81.9 \pm 0.3
Pets	88.7 \pm 0.2	89.9 \pm 0.2	90.7 \pm 0.3
Sun397	53.9 \pm 1.1	56.9 \pm 1.2	58.4 \pm 0.6
SVHN	24.5 \pm 0.4	36.8 \pm 0.6	40.8 \pm 0.8
DTD	58.5 \pm 0.0	61.1 \pm 0.0	65.3 \pm 0.3
EuroSAT	82.4 \pm 0.3	88.1 \pm 0.1	93.2 \pm 0.2
Resiscs45	67.1 \pm 0.2	74.6 \pm 0.2	81.8 \pm 0.4
Patch Camelyon	72.9 \pm 0.0	79.1 \pm 0.0	79.7 \pm 0.5
Retinopathy	33.0 \pm 0.3	40.4 \pm 0.3	46.9 \pm 0.4
CLEVR-count	28.9 \pm 0.3	40.1 \pm 0.4	50.3 \pm 0.3
CLEVR-dist	29.2 \pm 0.5	38.7 \pm 0.4	45.5 \pm 1.3
dSprites-loc	14.6 \pm 0.6	20.9 \pm 0.7	30.8 \pm 1.4
dSprites-ori	15.5 \pm 0.4	22.5 \pm 0.6	33.3 \pm 0.9
SmallNORB-azi	11.5 \pm 0.5	14.1 \pm 0.7	14.2 \pm 0.7
SmallNORB-elev	19.3 \pm 0.4	24.1 \pm 0.5	26.3 \pm 0.8
DMLab	35.4 \pm 0.4	39.7 \pm 0.3	44.4 \pm 0.4
KITTI-dist	53.4 \pm 0.0	66.7 \pm 0.0	69.8 \pm 0.4
FGVC-Aircraft	31.8 \pm 0.0	41.3 \pm 0.0	45.8 \pm 0.4
Cars	33.7 \pm 0.0	43.3 \pm 0.0	46.6 \pm 0.3
Letters	44.9 \pm 1.3	59.7 \pm 0.5	69.5 \pm 0.5
Average acc	46.4	53.4	58.0

Table 14. Accuracy comparison between NCM, LDA, and Linear head without using any adaptation (NA method). The reported results are based on the full training dataset and averaged over 5 runs (mean \pm std). A pre-trained EfficientNet-B0 is used as a backbone in all cases.

Dataset	NCM	LDA	Linear
Caltech101	86.6 \pm 0.5	89.0 \pm 0.6	88.5 \pm 0.4
CIFAR100	47.4 \pm 1.2	51.8 \pm 1.3	50.3 \pm 1.4
Flowers102	80.2 \pm 0.4	85.0 \pm 0.8	83.5 \pm 0.5
Pets	81.8 \pm 1.5	81.8 \pm 1.7	82.6 \pm 1.6
Sun397	40.9 \pm 0.7	40.9 \pm 0.7	38.1 \pm 1.0
SVHN	28.6 \pm 3.8	31.7 \pm 3.7	30.1 \pm 4.5
DTD	49.6 \pm 1.5	50.2 \pm 0.9	50.8 \pm 1.3
EuroSAT	75.8 \pm 1.5	78.1 \pm 1.2	78.3 \pm 1.2
Resiscs45	62.7 \pm 1.1	64.7 \pm 1.2	65.8 \pm 0.7
Patch Camelyon	64.7 \pm 5.8	64.9 \pm 6.6	62.9 \pm 5.4
Retinopathy	27.4 \pm 3.1	26.0 \pm 2.0	25.2 \pm 2.4
CLEVR-count	24.0 \pm 1.3	23.4 \pm 1.4	23.2 \pm 0.7
CLEVR-dist	23.1 \pm 1.4	23.1 \pm 1.1	24.0 \pm 1.3
dSprites-loc	19.5 \pm 1.8	19.8 \pm 2.0	16.7 \pm 5.9
dSprites-ori	20.6 \pm 1.6	26.5 \pm 0.8	25.5 \pm 1.4
SmallNORB-azi	9.0 \pm 1.0	10.1 \pm 0.6	10.3 \pm 0.6
SmallNORB-elev	14.6 \pm 0.9	15.4 \pm 0.7	15.5 \pm 0.8
DMLab	23.4 \pm 2.3	23.3 \pm 1.9	24.8 \pm 0.9
KITTI-dist	55.7 \pm 3.6	52.7 \pm 3.5	53.2 \pm 1.8
FGVC-Aircraft	28.7 \pm 0.7	32.6 \pm 0.9	33.1 \pm 1.3
Cars	22.7 \pm 0.5	28.1 \pm 0.4	27.2 \pm 0.7
Letters	52.2 \pm 2.9	55.9 \pm 2.5	56.4 \pm 3.2
Average acc	42.7	44.3	43.9

Table 15. Accuracy comparison between NCM, LDA, and Linear head using FiLM adaptation (**A-FiLM** method). The reported results are based on **5** shots and averaged over 5 runs (mean \pm std). A pre-trained EfficientNet-B0 is used as a backbone in all cases.

Dataset	NCM	LDA	Linear
Caltech101	89.9 \pm 0.2	91.5 \pm 0.4	91.1 \pm 0.6
CIFAR100	59.2 \pm 1.7	62.8 \pm 1.1	60.6 \pm 0.5
Flowers102	86.2 \pm 0.5	91.1 \pm 0.3	91.2 \pm 0.3
Pets	85.8 \pm 1.0	86.3 \pm 0.8	86.6 \pm 0.8
Sun397	48.5 \pm 0.8	49.3 \pm 0.6	44.8 \pm 1.2
SVHN	40.3 \pm 2.5	45.3 \pm 3.0	43.9 \pm 3.3
DTD	58.3 \pm 0.8	59.1 \pm 0.8	59.2 \pm 1.1
EuroSAT	81.9 \pm 1.4	84.4 \pm 1.6	83.5 \pm 0.7
Resiscs45	70.2 \pm 1.1	73.0 \pm 1.3	73.5 \pm 0.7
Patch Camelyon	69.2 \pm 5.2	68.5 \pm 6.1	67.1 \pm 4.8
Retinopathy	26.7 \pm 1.3	26.9 \pm 1.1	25.6 \pm 1.0
CLEVR-count	30.1 \pm 1.9	27.6 \pm 1.6	29.2 \pm 1.2
CLEVR-dist	25.3 \pm 1.7	26.2 \pm 1.3	26.5 \pm 0.7
dSprites-loc	26.2 \pm 11.4	26.1 \pm 10.6	24.2 \pm 14.7
dSprites-ori	26.7 \pm 2.4	34.0 \pm 2.6	33.8 \pm 2.4
SmallNORB-azi	11.0 \pm 0.8	11.7 \pm 1.2	11.3 \pm 1.4
SmallNORB-elev	15.6 \pm 0.7	16.3 \pm 0.4	16.6 \pm 0.3
DMLab	27.2 \pm 1.9	26.6 \pm 1.5	29.3 \pm 1.7
KITTI-dist	56.7 \pm 3.7	55.4 \pm 3.7	56.2 \pm 4.5
FGVC-Aircraft	37.5 \pm 0.7	43.3 \pm 1.1	43.4 \pm 1.5
Cars	36.3 \pm 0.8	43.1 \pm 1.0	42.1 \pm 1.0
Letters	64.0 \pm 1.5	67.5 \pm 1.3	68.1 \pm 1.4
Average acc	48.8	50.7	50.4

Table 16. Accuracy comparison between NCM, LDA, and Linear head using FiLM adaptation (**A-FiLM** method). The reported results are based on **10** shots and averaged over 5 runs (mean \pm std). A pre-trained EfficientNet-B0 is used as a backbone in all cases.

Dataset	NCM	LDA	Linear
Caltech101	93.4 \pm 0.7	93.8 \pm 0.5	93.5 \pm 1.0
CIFAR100	72.6 \pm 0.7	73.8 \pm 0.9	73.7 \pm 0.5
Flowers102	86.2 \pm 0.5	91.1 \pm 0.3	91.2 \pm 0.3
Pets	89.3 \pm 0.6	89.9 \pm 0.7	89.9 \pm 0.7
Sun397	58.5 \pm 0.7	59.7 \pm 0.6	60.8 \pm 0.7
SVHN	73.9 \pm 1.1	77.2 \pm 0.8	76.8 \pm 1.0
DTD	66.8 \pm 0.3	68.4 \pm 0.2	68.7 \pm 0.7
EuroSAT	91.0 \pm 0.6	93.0 \pm 0.6	93.2 \pm 0.6
Resics45	81.7 \pm 0.2	83.4 \pm 0.6	85.3 \pm 0.6
Patch Camelyon	78.5 \pm 2.0	77.9 \pm 2.4	78.1 \pm 2.4
Retinopathy	34.2 \pm 1.6	35.2 \pm 1.2	33.5 \pm 1.9
CLEVR-count	56.8 \pm 0.9	46.6 \pm 1.1	53.1 \pm 1.1
CLEVR-dist	40.2 \pm 1.8	38.8 \pm 1.0	41.2 \pm 1.5
dSprites-loc	83.6 \pm 5.4	83.7 \pm 5.6	81.6 \pm 5.9
dSprites-ori	41.2 \pm 0.8	52.1 \pm 1.3	53.8 \pm 1.4
SmallNORB-azi	17.0 \pm 0.8	16.8 \pm 0.8	17.5 \pm 1.0
SmallNORB-elev	23.1 \pm 1.2	22.9 \pm 0.5	24.0 \pm 0.6
DMLab	35.0 \pm 0.6	34.6 \pm 0.6	35.8 \pm 0.4
KITTI-dist	67.3 \pm 2.1	66.8 \pm 3.0	66.5 \pm 2.7
FGVC-Aircraft	60.6 \pm 0.9	65.1 \pm 0.7	68.0 \pm 0.6
Cars	60.9 \pm 0.2	67.9 \pm 0.2	74.5 \pm 0.4
Letters	76.7 \pm 0.5	79.7 \pm 0.4	81.9 \pm 0.8
Average acc	63.1	64.5	65.6

Table 17. Accuracy comparison between NCM, LDA, and Linear head using FiLM adaptation (**A-FiLM** method). The reported results are based on **50** shots and averaged over 5 runs (mean \pm std). A pre-trained EfficientNet-B0 is used as a backbone in all cases.

Dataset	NCM	LDA	Linear
Caltech101	93.6 \pm 0.4	94.4 \pm 0.3	94.1 \pm 0.6
CIFAR100	77.4 \pm 1.1	78.2 \pm 1.1	82.1 \pm 1.1
Flowers102	88.6 \pm 0.6	91.2 \pm 0.4	90.6 \pm 0.5
Pets	90.2 \pm 0.2	90.8 \pm 0.3	91.0 \pm 0.4
Sun397	61.4 \pm 0.5	62.1 \pm 0.3	63.7 \pm 0.9
SVHN	92.9 \pm 0.4	93.1 \pm 0.4	95.1 \pm 0.4
DTD	64.8 \pm 0.2	66.8 \pm 0.5	67.6 \pm 0.6
EuroSAT	96.5 \pm 0.3	97.2 \pm 0.1	98.1 \pm 0.3
Resics45	88.0 \pm 0.3	89.4 \pm 0.4	94.2 \pm 0.4
Patch Camelyon	84.3 \pm 1.5	85.9 \pm 1.2	85.8 \pm 1.6
Retinopathy	52.3 \pm 0.7	52.6 \pm 0.8	59.5 \pm 0.8
CLEVR-count	94.5 \pm 0.2	93.5 \pm 0.7	95.3 \pm 0.6
CLEVR-dist	79.3 \pm 1.4	80.1 \pm 2.3	84.5 \pm 2.0
dSprites-loc	98.0 \pm 0.5	98.5 \pm 0.6	99.3 \pm 0.4
dSprites-ori	69.8 \pm 2.4	80.0 \pm 0.8	90.7 \pm 0.8
SmallNORB-azi	26.1 \pm 1.2	24.4 \pm 0.6	23.5 \pm 0.5
SmallNORB-elev	47.0 \pm 0.9	47.9 \pm 1.2	47.9 \pm 1.4
DMLab	60.2 \pm 0.6	61.3 \pm 0.5	65.8 \pm 1.0
KITTI-dist	78.5 \pm 0.9	80.1 \pm 1.1	79.7 \pm 0.4
FGVC-Aircraft	63.3 \pm 0.2	67.5 \pm 0.4	71.5 \pm 0.5
Cars	60.1 \pm 0.1	67.3 \pm 0.3	73.6 \pm 0.3
Letters	77.1 \pm 0.3	81.7 \pm 0.4	85.2 \pm 0.3
Average acc	74.7	76.6	79.0

Table 18. Accuracy comparison between NCM, LDA, and Linear head using FiLM adaptation (**A-FiLM** method). The reported results are based on the full training dataset and averaged over 5 runs (mean \pm std). A pre-trained EfficientNet-B0 is used as a backbone in all cases.

Dataset	NCM	LDA	Linear
Caltech101	87.1 \pm 0.6	89.4 \pm 0.7	86.1 \pm 0.9
CIFAR100	48.1 \pm 0.7	49.3 \pm 1.1	49.2 \pm 1.0
Flowers102	81.5 \pm 0.8	81.7 \pm 0.6	83.6 \pm 0.8
Pets	80.9 \pm 1.7	80.8 \pm 1.7	71.1 \pm 1.2
Sun397	35.5 \pm 0.3	35.2 \pm 0.5	37.2 \pm 0.3
SVHN	19.1 \pm 1.5	19.6 \pm 1.2	19.2 \pm 1.8
DTD	48.4 \pm 1.3	49.0 \pm 1.3	41.6 \pm 0.8
EuroSAT	75.4 \pm 4.1	76.7 \pm 2.9	78.5 \pm 1.2
Resiscs45	61.7 \pm 2.3	62.3 \pm 2.5	63.5 \pm 2.5
Patch Camelyon	59.2 \pm 4.9	59.4 \pm 4.9	60.5 \pm 7.0
Retinopathy	24.6 \pm 2.7	24.5 \pm 2.5	26.1 \pm 2.4
CLEVR-count	23.9 \pm 2.9	23.5 \pm 3.0	24.2 \pm 3.1
CLEVR-dist	25.1 \pm 3.3	25.6 \pm 3.5	25.6 \pm 2.4
dSprites-loc	26.1 \pm 2.7	27.1 \pm 1.6	25.5 \pm 3.6
dSprites-ori	18.3 \pm 1.6	19.9 \pm 1.5	15.6 \pm 1.9
SmallNORB-azi	10.0 \pm 0.7	10.4 \pm 0.8	10.3 \pm 0.9
SmallNORB-elev	15.8 \pm 1.1	16.2 \pm 1.1	15.6 \pm 0.8
DMLab	21.3 \pm 1.6	22.1 \pm 1.3	22.6 \pm 0.9
KITTI-dist	51.1 \pm 2.5	52.8 \pm 2.5	52.1 \pm 2.0
FGVC-Aircraft	23.8 \pm 0.7	23.6 \pm 0.8	25.1 \pm 1.0
Cars	23.1 \pm 0.3	23.5 \pm 0.3	25.3 \pm 0.5
Letters	35.5 \pm 3.3	35.7 \pm 3.3	37.0 \pm 3.2
Average acc	40.7	41.3	40.7

Table 19. Accuracy comparison between NCM, LDA, and Linear head using full-body adaptation (**A-FB** method). The reported results are based on **5** shots and averaged over 5 runs (mean \pm std). A pre-trained EfficientNet-B0 is used as a backbone in all cases.

Dataset	NCM	LDA	Linear
Caltech101	90.4 \pm 0.8	91.7 \pm 0.7	89.3 \pm 0.8
CIFAR100	58.8 \pm 0.4	59.5 \pm 0.3	59.5 \pm 0.8
Flowers102	89.9 \pm 0.6	90.0 \pm 0.5	91.3 \pm 0.6
Pets	85.5 \pm 0.9	85.7 \pm 0.5	78.4 \pm 1.7
Sun397	45.2 \pm 0.7	45.0 \pm 0.4	46.3 \pm 0.3
SVHN	26.4 \pm 3.4	27.1 \pm 3.8	26.4 \pm 3.6
DTD	55.2 \pm 0.8	56.7 \pm 1.0	48.0 \pm 0.8
EuroSAT	83.9 \pm 1.5	84.9 \pm 1.5	86.3 \pm 1.5
Resiscs45	72.6 \pm 1.2	72.8 \pm 1.3	74.3 \pm 1.1
Patch Camelyon	61.3 \pm 4.5	61.2 \pm 4.5	63.0 \pm 5.1
Retinopathy	25.1 \pm 4.2	24.6 \pm 3.3	27.5 \pm 2.0
CLEVR-count	28.0 \pm 1.9	27.7 \pm 2.0	28.7 \pm 2.1
CLEVR-dist	30.1 \pm 4.1	30.0 \pm 4.2	29.9 \pm 3.6
dSprites-loc	42.9 \pm 2.7	44.8 \pm 1.3	42.2 \pm 3.1
dSprites-ori	26.4 \pm 6.5	29.6 \pm 6.8	22.9 \pm 10.4
SmallNORB-azi	12.2 \pm 0.6	11.5 \pm 0.8	11.7 \pm 0.6
SmallNORB-elev	18.2 \pm 1.3	18.3 \pm 1.5	17.3 \pm 1.1
DMLab	25.3 \pm 1.2	25.6 \pm 1.3	26.1 \pm 1.1
KITTI-dist	53.5 \pm 2.3	54.9 \pm 1.3	52.2 \pm 2.1
FGVC-Aircraft	37.4 \pm 0.5	36.7 \pm 0.6	38.6 \pm 0.4
Cars	43.8 \pm 0.8	43.5 \pm 0.6	46.9 \pm 0.8
Letters	55.8 \pm 1.5	55.2 \pm 1.3	56.6 \pm 1.4
Average acc	48.5	49.0	48.3

Table 20. Accuracy comparison between NCM, LDA, and Linear head using full-body adaptation (**A-FB** method). The reported results are based on **10** shots and averaged over 5 runs (mean \pm std). A pre-trained EfficientNet-B0 is used as a backbone in all cases.

Dataset	NCM	LDA	Linear
Caltech101	92.8 \pm 0.3	93.9 \pm 0.3	92.6 \pm 0.5
CIFAR100	72.9 \pm 0.9	73.1 \pm 0.7	72.7 \pm 0.8
Flowers102	89.9 \pm 0.6	90.0 \pm 0.5	91.3 \pm 0.6
Pets	88.7 \pm 0.5	89.6 \pm 0.6	84.9 \pm 1.1
Sun397	59.9 \pm 0.6	60.4 \pm 0.6	62.4 \pm 0.4
SVHN	63.9 \pm 1.5	64.5 \pm 1.3	64.6 \pm 1.6
DTD	60.9 \pm 0.3	64.4 \pm 0.2	57.4 \pm 0.7
EuroSAT	93.8 \pm 0.5	94.1 \pm 0.6	93.9 \pm 1.0
Resics45	87.4 \pm 0.8	87.6 \pm 0.7	88.0 \pm 0.8
Patch Camelyon	71.6 \pm 1.7	72.2 \pm 1.8	74.4 \pm 1.8
Retinopathy	31.1 \pm 3.3	31.3 \pm 2.9	31.9 \pm 2.2
CLEVR-count	46.5 \pm 1.0	45.2 \pm 1.1	45.4 \pm 1.9
CLEVR-dist	44.0 \pm 2.1	44.7 \pm 2.2	45.7 \pm 2.2
dSprites-loc	85.3 \pm 4.0	87.1 \pm 2.4	85.2 \pm 3.2
dSprites-ori	42.6 \pm 3.2	44.8 \pm 2.3	39.3 \pm 4.7
SmallNORB-azi	19.6 \pm 0.6	18.3 \pm 0.7	19.1 \pm 1.1
SmallNORB-elev	31.4 \pm 1.4	31.3 \pm 1.7	31.3 \pm 2.1
DMLab	32.6 \pm 1.4	32.7 \pm 1.6	34.0 \pm 0.9
KITTI-dist	65.8 \pm 2.1	66.9 \pm 2.2	65.8 \pm 1.8
FGVC-Aircraft	74.2 \pm 0.8	73.5 \pm 0.4	74.6 \pm 0.3
Cars	79.3 \pm 0.1	79.4 \pm 0.1	81.5 \pm 0.2
Letters	82.1 \pm 0.7	82.3 \pm 0.9	83.1 \pm 0.6
Average acc	64.4	64.9	64.5

Table 21. Accuracy comparison between NCM, LDA, and Linear head using full-body adaptation (**A-FB** method). The reported results are based on **50** shots and averaged over 5 runs (mean \pm std). A pre-trained EfficientNet-B0 is used as a backbone in all cases.

Dataset	NCM	LDA	Linear
Caltech101	94.2 \pm 0.5	94.6 \pm 0.3	94.8 \pm 0.3
CIFAR100	84.2 \pm 1.2	84.3 \pm 0.9	85.0 \pm 1.1
Flowers102	90.3 \pm 0.3	90.3 \pm 0.4	91.4 \pm 0.5
Pets	89.7 \pm 0.4	89.5 \pm 0.3	90.0 \pm 0.4
Sun397	65.9 \pm 0.3	66.1 \pm 1.0	66.7 \pm 0.4
SVHN	95.6 \pm 0.2	95.3 \pm 0.5	95.5 \pm 0.3
DTD	67.6 \pm 0.8	68.1 \pm 0.4	68.5 \pm 0.5
EuroSAT	98.1 \pm 0.2	98.5 \pm 0.3	98.6 \pm 0.2
Resics45	95.3 \pm 0.1	95.5 \pm 0.2	95.9 \pm 0.1
Patch Camelyon	81.1 \pm 2.2	85.0 \pm 0.7	86.5 \pm 0.9
Retinopathy	55.8 \pm 0.9	56.1 \pm 1.4	57.7 \pm 0.7
CLEVR-count	98.5 \pm 0.3	98.7 \pm 0.3	98.3 \pm 0.3
CLEVR-dist	89.0 \pm 0.6	89.0 \pm 0.6	89.4 \pm 1.5
dSprites-loc	99.7 \pm 0.3	99.8 \pm 0.1	99.6 \pm 0.4
dSprites-ori	89.2 \pm 1.0	94.0 \pm 0.7	93.0 \pm 1.1
SmallNORB-azi	29.8 \pm 1.0	28.7 \pm 0.6	28.9 \pm 0.8
SmallNORB-elev	74.3 \pm 4.3	81.8 \pm 3.1	77.2 \pm 4.6
DMLab	64.8 \pm 0.6	65.7 \pm 0.4	65.6 \pm 0.7
KITTI-dist	78.2 \pm 0.7	82.1 \pm 0.6	82.3 \pm 1.1
FGVC-Aircraft	76.0 \pm 0.5	75.8 \pm 0.7	76.7 \pm 0.8
Cars	79.1 \pm 0.1	78.9 \pm 0.2	81.3 \pm 0.2
Letters	86.0 \pm 0.5	85.7 \pm 0.5	87.2 \pm 0.3
Average acc	81.0	82.0	82.3

Table 22. Accuracy comparison between NCM, LDA, and Linear head using full-body adaptation (**A-FB** method). The reported results are based on the full training dataset and averaged over 5 runs (mean \pm std). A pre-trained EfficientNet-B0 is used as a backbone in all cases.

Dataset	NA(RN)	FiLM(RN)	NA(EN)	FiLM(EN)
Caltech101	80.9 ±0.7	81.1 ±0.7	88.2 ±0.8	89.0 ±0.6
CIFAR100	40.4 ±0.5	42.2 ±0.9	42.7 ±1.6	51.8 ±1.3
Flowers102	72.6 ±0.8	79.4 ±1.4	76.1 ±0.4	85.0 ±0.8
Pets	76.9 ±1.2	74.5 ±1.4	82.4 ±1.6	81.8 ±1.7
Sun397	35.1 ±0.9	29.1 ±0.7	41.9 ±1.0	40.9 ±0.7
SVHN	20.9 ±1.3	28.8 ±2.7	16.5 ±1.1	31.7 ±3.7
DTD	43.2 ±1.7	42.2 ±0.7	48.9 ±1.7	50.2 ±0.9
EuroSAT	75.1 ±1.9	79.3 ±1.2	76.3 ±1.8	78.1 ±1.2
Resiscs45	56.8 ±1.3	57.0 ±1.2	58.8 ±1.4	64.7 ±1.2
Patch Camelyon	62.4 ±5.5	64.6 ±7.2	59.8 ±7.2	64.9 ±6.6
Retinopathy	23.0 ±2.5	23.6 ±1.7	25.6 ±1.6	26.0 ±2.0
CLEVR-count	21.6 ±1.7	23.0 ±1.3	23.1 ±1.1	23.4 ±1.4
CLEVR-dist	22.9 ±1.4	24.4 ±1.3	24.5 ±2.3	23.1 ±1.1
dSprites-loc	13.0 ±1.0	15.9 ±1.0	8.5 ±0.6	19.8 ±2.0
dSprites-ori	14.4 ±0.6	22.9 ±0.8	16.2 ±0.8	26.5 ±0.8
SmallNORB-azi	9.4 ±0.8	9.8 ±1.1	9.3 ±0.8	10.1 ±0.6
SmallNORB-elev	15.8 ±0.7	15.9 ±0.7	15.1 ±0.6	15.4 ±0.7
DMLab	21.6 ±1.5	22.1 ±1.8	22.1 ±1.3	23.3 ±1.9
KITTI-dist	54.3 ±2.8	54.0 ±2.5	51.4 ±2.7	52.7 ±3.5
FGVC-Aircraft	19.1 ±0.9	20.3 ±0.7	22.1 ±1.0	32.6 ±0.9
Cars	14.8 ±0.5	13.9 ±0.3	22.6 ±0.6	28.1 ±0.4
Letters	32.4 ±1.9	45.5 ±2.4	36.1 ±2.1	55.9 ±2.5
Average acc	37.6	39.5	39.5	44.3

Table 23. Accuracy comparison between NA and FiLM methods in offline mode using either a pre-trained ResNet-18 (RN) or a pre-trained EfficientNet-B0 (EN) backbone. We use an LDA head. The reported results are based on **5** shots. Results are averaged over 5 runs (mean±std).

Dataset	NA(RN)	FiLM(RN)	NA(EN)	FiLM(EN)
Caltech101	85.0 ±0.6	86.6 ±0.6	90.0 ±0.8	91.5 ±0.4
CIFAR100	48.5 ±0.4	52.2 ±0.8	50.1 ±1.5	62.8 ±1.1
Flowers102	81.2 ±0.7	87.1 ±0.2	83.9 ±0.3	91.1 ±0.3
Pets	82.3 ±0.7	80.5 ±1.1	86.4 ±0.7	86.3 ±0.8
Sun397	42.8 ±0.9	36.3 ±1.0	49.0 ±1.3	49.3 ±0.6
SVHN	24.6 ±1.7	35.8 ±4.1	19.4 ±2.9	45.3 ±3.0
DTD	51.9 ±0.9	50.5 ±0.6	55.6 ±0.6	59.1 ±0.8
EuroSAT	82.0 ±0.7	85.4 ±0.9	82.1 ±0.9	84.4 ±1.6
Resiscs45	64.8 ±1.5	67.2 ±2.0	65.5 ±1.1	73.0 ±1.3
Patch Camelyon	66.9 ±3.7	68.8 ±3.7	66.5 ±3.7	68.5 ±6.1
Retinopathy	25.5 ±1.3	25.8 ±3.7	27.1 ±2.2	26.9 ±1.1
CLEVR-count	23.8 ±0.7	25.6 ±2.0	25.7 ±0.6	27.6 ±1.6
CLEVR-dist	24.9 ±0.7	27.2 ±1.2	26.3 ±1.1	26.2 ±1.3
dSprites-loc	14.7 ±0.4	25.4 ±1.5	8.7 ±0.3	26.1 ±10.6
dSprites-ori	16.6 ±0.9	29.7 ±1.3	18.2 ±0.7	34.0 ±2.6
SmallNORB-azi	10.4 ±0.9	12.2 ±1.1	9.5 ±1.1	11.7 ±1.2
SmallNORB-elev	16.9 ±0.8	17.2 ±1.1	16.5 ±1.1	16.3 ±0.4
DMLab	24.6 ±1.8	25.6 ±1.4	25.7 ±1.2	26.6 ±1.5
KITTI-dist	53.0 ±2.0	55.9 ±3.5	52.9 ±1.5	55.4 ±3.7
FGVC-Aircraft	25.9 ±0.8	29.5 ±0.8	28.5 ±0.4	43.3 ±1.1
Cars	21.5 ±0.5	24.0 ±0.2	30.4 ±0.5	43.1 ±1.0
Letters	41.5 ±1.2	62.7 ±1.9	45.6 ±0.8	67.5 ±1.3
Average acc	42.2	46.0	43.8	50.7

Table 24. Accuracy comparison between NA and FiLM methods in offline mode using either a pre-trained ResNet-18 (RN) or a pre-trained EfficientNet-B0 (EN) backbone. We use an LDA head. The reported results are based on **10** shots. Results are averaged over 5 runs (mean±std).

Dataset	NA(RN)	FiLM(RN)	NA(EN)	FiLM(EN)
Caltech101	88.0 ±0.3	87.7 ±0.7	91.9 ±0.5	93.8 ±0.5
CIFAR100	58.2 ±0.9	61.8 ±0.7	57.4 ±1.0	73.8 ±0.9
Flowers102	81.2 ±0.7	87.1 ±0.2	83.9 ±0.3	91.1 ±0.3
Pets	86.9 ±0.4	86.8 ±0.6	89.5 ±0.4	89.9 ±0.7
Sun397	51.4 ±1.3	47.8 ±0.9	55.9 ±1.0	59.7 ±0.6
SVHN	37.3 ±0.8	74.5 ±0.9	28.3 ±1.1	77.2 ±0.8
DTD	59.9 ±0.0	59.3 ±0.6	61.1 ±0.0	68.4 ±0.2
EuroSAT	88.3 ±0.5	92.6 ±0.5	87.7 ±0.9	93.0 ±0.6
Resics45	73.7 ±1.1	77.5 ±1.1	73.5 ±0.9	83.4 ±0.6
Patch Camelyon	76.3 ±0.9	77.4 ±1.1	76.2 ±1.1	77.9 ±2.4
Retinopathy	29.2 ±2.1	30.4 ±1.0	32.9 ±2.2	35.2 ±1.2
CLEVR-count	29.5 ±1.3	39.9 ±1.4	30.1 ±1.0	46.6 ±1.1
CLEVR-dist	31.7 ±0.8	45.3 ±2.6	32.2 ±1.1	38.8 ±1.0
dSprites-loc	21.8 ±0.6	70.2 ±2.0	11.9 ±0.4	83.7 ±5.6
dSprites-ori	20.8 ±0.4	52.1 ±1.5	20.1 ±1.1	52.1 ±1.3
SmallNORB-azi	13.9 ±0.5	16.4 ±0.7	12.3 ±0.8	16.8 ±0.8
SmallNORB-elev	21.4 ±1.0	25.1 ±0.6	19.1 ±0.7	22.9 ±0.5
DMLab	29.7 ±0.5	31.6 ±0.9	30.6 ±0.3	34.6 ±0.6
KITTI-dist	62.0 ±3.5	66.0 ±2.7	61.4 ±2.3	66.8 ±3.0
FGVC-Aircraft	38.9 ±0.5	53.1 ±0.3	41.0 ±0.7	65.1 ±0.7
Cars	34.4 ±0.0	49.5 ±0.2	43.3 ±0.0	67.9 ±0.2
Letters	56.1 ±1.2	77.7 ±1.3	57.6 ±0.8	79.7 ±0.4
Average acc	49.6	59.5	49.9	64.5

Table 25. Accuracy comparison between NA and FiLM methods in offline mode using either a pre-trained ResNet-18 (RN) or a pre-trained EfficientNet-B0 (EN) backbone. We use an LDA head. The reported results are based on **50** shots. Results are averaged over 5 runs (mean±std).

Dataset	NA	Meta-Learn	FiLM	Full-body
Caltech101	88.2 ±0.8	86.7 ±0.9	89.0 ±0.6	89.4 ±0.7
CIFAR100	42.7 ±1.6	42.1 ±1.3	51.8 ±1.3	49.3 ±1.1
Flowers102	76.1 ±0.4	78.2 ±0.4	85.0 ±0.8	81.7 ±0.6
Pets	82.4 ±1.6	83.8 ±1.0	81.8 ±1.7	80.8 ±1.7
Sun397	41.9 ±1.0	40.2 ±0.6	40.9 ±0.7	35.2 ±0.5
SVHN	16.5 ±1.1	27.4 ±3.6	31.7 ±3.7	19.6 ±1.2
DTD	48.9 ±1.7	50.5 ±1.7	50.2 ±0.9	49.0 ±1.3
EuroSAT	76.3 ±1.8	75.2 ±1.5	78.1 ±1.2	76.7 ±2.9
Resics45	58.8 ±1.4	62.7 ±1.0	64.7 ±1.2	62.3 ±2.5
Patch Camelyon	59.8 ±7.2	64.2 ±7.3	64.9 ±6.6	59.4 ±4.9
Retinopathy	25.6 ±1.6	26.8 ±3.5	26.0 ±2.0	24.5 ±2.5
CLEVR-count	23.1 ±1.1	22.6 ±0.8	23.4 ±1.4	23.5 ±3.0
CLEVR-dist	24.5 ±2.3	23.8 ±1.1	23.1 ±1.1	25.6 ±3.5
dSprites-loc	8.5 ±0.6	8.9 ±0.5	19.8 ±2.0	27.1 ±1.6
dSprites-ori	16.2 ±0.8	19.2 ±0.7	26.5 ±0.8	19.9 ±1.5
SmallNORB-azi	9.3 ±0.8	8.7 ±1.0	10.1 ±0.6	10.4 ±0.8
SmallNORB-elev	15.1 ±0.6	15.4 ±0.5	15.4 ±0.7	16.2 ±1.1
DMLab	22.1 ±1.3	24.9 ±1.5	23.3 ±1.9	22.1 ±1.3
KITTI-dist	51.4 ±2.7	55.0 ±1.5	52.7 ±3.5	52.8 ±2.5
FGVC-Aircraft	22.1 ±1.0	31.9 ±0.6	32.6 ±0.9	23.6 ±0.8
Cars	22.6 ±0.6	22.8 ±0.4	28.1 ±0.4	23.5 ±0.3
Letters	36.1 ±2.1	46.5 ±3.2	55.9 ±2.5	35.7 ±3.3
Average acc	39.5	41.7	44.3	41.3

Table 26. Accuracy comparison between different adaptation methods in offline mode using a pre-trained EfficientNet-B0 backbone. We use an LDA head. The reported results are based on **5** shots and averaged over 5 runs (mean±std).

Dataset	NA	Meta-Learn	FiLM	Full-body
Caltech101	90.0 ±0.8	89.1 ±0.3	91.5 ±0.4	91.7 ±0.7
CIFAR100	50.1 ±1.5	50.1 ±1.2	62.8 ±1.1	59.5 ±0.3
Flowers102	83.9 ±0.3	84.4 ±0.3	91.1 ±0.3	90.0 ±0.5
Pets	86.4 ±0.7	86.8 ±0.2	86.3 ±0.8	85.7 ±0.5
Sun397	49.0 ±1.3	46.3 ±0.9	49.3 ±0.6	45.0 ±0.4
SVHN	19.4 ±2.9	33.0 ±2.2	45.3 ±3.0	27.1 ±3.8
DTD	55.6 ±0.6	57.7 ±1.4	59.1 ±0.8	56.7 ±1.0
EuroSAT	82.1 ±0.9	81.2 ±0.7	84.4 ±1.6	84.9 ±1.5
Resics45	65.5 ±1.1	68.4 ±1.2	73.0 ±1.3	72.8 ±1.3
Patch Camelyon	66.5 ±3.7	67.5 ±5.5	68.5 ±6.1	61.2 ±4.5
Retinopathy	27.1 ±2.2	26.9 ±0.4	26.9 ±1.1	24.6 ±3.3
CLEVR-count	25.7 ±0.6	24.3 ±1.1	27.6 ±1.6	27.7 ±2.0
CLEVR-dist	26.3 ±1.1	25.5 ±0.8	26.2 ±1.3	30.0 ±4.2
dSprites-loc	8.7 ±0.3	8.9 ±0.4	26.1 ±10.6	44.8 ±1.3
dSprites-ori	18.2 ±0.7	20.4 ±1.2	34.0 ±2.6	29.6 ±6.8
SmallNORB-azi	9.5 ±1.1	10.5 ±0.2	11.7 ±1.2	11.5 ±0.8
SmallNORB-elev	16.5 ±1.1	15.8 ±0.6	16.3 ±0.4	18.3 ±1.5
DMLab	25.7 ±1.2	27.8 ±1.7	26.6 ±1.5	25.6 ±1.3
KITTI-dist	52.9 ±1.5	56.4 ±1.8	55.4 ±3.7	54.9 ±1.3
FGVC-Aircraft	28.5 ±0.4	39.0 ±0.8	43.3 ±1.1	36.7 ±0.6
Cars	30.4 ±0.5	29.8 ±0.1	43.1 ±1.0	43.5 ±0.6
Letters	45.6 ±0.8	54.5 ±1.5	67.5 ±1.3	55.2 ±1.3
Average acc	43.8	45.7	50.7	49.0

Table 27. Accuracy comparison between different adaptation methods in offline mode using a pre-trained EfficientNet-B0 backbone. We use an LDA head. The reported results are based on **10** shots and averaged over 5 runs (mean±std).

Dataset	NA	Meta-Learn	FiLM	Full-body
Caltech101	91.9 \pm 0.5	91.0 \pm 0.4	93.8 \pm 0.5	93.9 \pm 0.3
CIFAR100	57.4 \pm 1.0	58.0 \pm 0.9	73.8 \pm 0.9	73.1 \pm 0.7
Flowers102	83.9 \pm 0.3	84.4 \pm 0.3	91.1 \pm 0.3	90.0 \pm 0.5
Pets	89.5 \pm 0.4	89.6 \pm 0.3	89.9 \pm 0.7	89.6 \pm 0.6
Sun397	55.9 \pm 1.0	53.7 \pm 0.8	59.7 \pm 0.6	60.4 \pm 0.6
SVHN	28.3 \pm 1.1	47.3 \pm 1.4	77.2 \pm 0.8	64.5 \pm 1.3
DTD	61.1 \pm 0.0	63.8 \pm 0.0	68.4 \pm 0.2	64.4 \pm 0.2
EuroSAT	87.7 \pm 0.9	85.7 \pm 0.6	93.0 \pm 0.6	94.1 \pm 0.6
Resisc45	73.5 \pm 0.9	75.5 \pm 1.0	83.4 \pm 0.6	87.6 \pm 0.7
Patch Camelyon	76.2 \pm 1.1	78.0 \pm 1.4	77.9 \pm 2.4	72.2 \pm 1.8
Retinopathy	32.9 \pm 2.2	31.6 \pm 1.2	35.2 \pm 1.2	31.3 \pm 2.9
CLEVR-count	30.1 \pm 1.0	28.7 \pm 1.1	46.6 \pm 1.1	45.2 \pm 1.1
CLEVR-dist	32.2 \pm 1.1	30.5 \pm 1.7	38.8 \pm 1.0	44.7 \pm 2.2
dSprites-loc	11.9 \pm 0.4	12.2 \pm 0.5	83.7 \pm 5.6	87.1 \pm 2.4
dSprites-ori	20.1 \pm 1.1	24.7 \pm 1.9	52.1 \pm 1.3	44.8 \pm 2.3
SmallNORB-azi	12.3 \pm 0.8	12.4 \pm 0.5	16.8 \pm 0.8	18.3 \pm 0.7
SmallNORB-elev	19.1 \pm 0.7	18.9 \pm 1.0	22.9 \pm 0.5	31.3 \pm 1.7
DMLab	30.6 \pm 0.3	32.6 \pm 0.8	34.6 \pm 0.6	32.7 \pm 1.6
KITTI-dist	61.4 \pm 2.3	62.6 \pm 2.0	66.8 \pm 3.0	66.9 \pm 2.2
FGVC-Aircraft	41.0 \pm 0.7	50.9 \pm 0.7	65.1 \pm 0.7	73.5 \pm 0.4
Cars	43.3 \pm 0.0	40.1 \pm 0.0	67.9 \pm 0.2	79.4 \pm 0.1
Letters	57.6 \pm 0.8	64.2 \pm 0.6	79.7 \pm 0.4	82.3 \pm 0.9
Average acc	49.9	51.7	64.5	64.9

Table 28. Accuracy comparison between different adaptation methods in offline mode using a pre-trained EfficientNet-B0 backbone. We use an LDA head. The reported results are based on **50** shots and averaged over 5 runs (mean \pm std).

Method	Accuracy (%) in each session (\uparrow)									
	1	2	3	4	5	6	7	8	9	10
NA	93.2	87.1	81.9	80.2	76.8	74.3	72.8	70.6	70.1	68.2
E-EWC+SDC	<u>97.2</u>	<u>70.5</u>	<u>63.6</u>	<u>46.4</u>	<u>40.2</u>	<u>40.7</u>	<u>38.8</u>	<u>35.5</u>	<u>33.9</u>	<u>32.4</u>
FACT	96.6	48.2	32.8	24.2	19.3	16.4	13.9	12.5	11.3	10.2
ALICE	96.6	80.2	73.7	69.4	64.8	61.7	58.1	55.7	54.3	52.4
FSA	96.0	86.3	80.5	77.7	74.2	70.9	68.2	65.8	64.2	62.8
FSA-LL	96.4	84.9	79.1	75.4	71.6	68.5	66.4	64.1	62.7	60.5
FSA-FiLM	96.4	90.4	86.8	84.7	82.0	79.8	78.2	76.1	75.7	73.8
GDumb-1k	94.17	86.2	81.0	76.1	70.8	64.3	62.0	59.7	57.1	54.5
GDumb-5k	97.0	91.6	88.1	85.1	81.8	77.9	75.6	73.2	71.8	69.3

Table 29. Detailed accuracy for each incremental session on **CIFAR100** under the **high-shot CIL** setting. The best results across all methods per session are in bold while the best results across the no-memory methods are underlined. A pre-trained EfficientNet-B0 on Imagenet-1k is used as a backbone for all methods.

Method	Accuracy (%) in each session (\uparrow)								
	1	2	3	4	5	6	7	8	9
NA	96.3	94.5	91.6	89.9	87.7	84.8	82.0	82.8	82.6
E-EWC+SDC	<u>98.7</u>	<u>89.7</u>	<u>72.6</u>	<u>65.4</u>	<u>43.0</u>	<u>40.8</u>	<u>35.1</u>	<u>26.6</u>	<u>21.7</u>
FACT	98.5	66.9	50.5	40.4	33.8	28.9	25.3	23.9	22.0
ALICE	98.1	92.2	87.0	84.4	80.4	76.4	72.6	73.4	72.8
FSA	98.0	93.6	89.8	88.8	86.8	84.4	81.7	82.3	82.8
FSA-LL	97.8	92.1	87.3	85.6	83.6	81.4	78.5	78.6	79.0
FSA-FiLM	98.5	96.0	92.6	90.6	89.5	87.3	85.0	85.6	85.4
GDumb-1k	96.9	94.3	91.9	90.6	88.2	85.4	80.7	82.3	82.4
GDumb-5k	97.5	96.7	94.6	92.7	91.8	90.3	89.0	90.0	90.0

Table 30. Detailed accuracy for each incremental session on **CORE50** under the **high-shot CIL** setting. The best results across all methods per session are in bold while the best results across the no-memory methods are underlined. A pre-trained EfficientNet-B0 on Imagenet-1k is used as a backbone for all methods.

Method	Accuracy (%) in each session (\uparrow)				
	1	2	3	4	5
NA	81.5	61.5	48.5	42.5	39.9
E-EWC+SDC	<u>99.0</u>	<u>55.5</u>	<u>48.1</u>	<u>44.7</u>	<u>39.5</u>
FACT	99.3	63.5	47.4	38.7	33.8
ALICE	99.3	73.5	56.4	49.9	46.1
FSA	97.2	86.4	78.2	73.0	71.3
FSA-LL	96.7	82.7	72.6	67.4	64.6
FSA-FiLM	99.1	89.0	81.7	77.6	75.9
GDumb-1k	97.4	91.7	87.3	83.8	78.3
GDumb-5k	98.6	97.3	95.8	93.7	93.2

Table 31. Detailed accuracy for each incremental session on **SVHN** under the **high-shot CIL** setting. The best results across all methods per session are in bold while the best results across the no-memory methods are underlined. A pre-trained EfficientNet-B0 on Imagenet-1k is used as a backbone for all methods.

Method	Accuracy (%) in each session (\uparrow)						
	1	2	3	4	5	6	7
NA	44.9	37.4	31.6	27.1	23.8	21.5	20.6
<u>E-EWC+SDC</u>	<u>99.5</u>	<u>58.1</u>	<u>29.9</u>	<u>33.0</u>	<u>19.4</u>	<u>21.7</u>	<u>18.6</u>
FACT	100.0	16.6	12.7	10.1	8.4	7.2	6.4
ALICE	100.0	92.6	77.6	69.6	65.6	69.8	68.3
FSA	100.0	95.4	92.3	87.7	89.9	90.7	91.5
FSA-LL	99.8	94.0	93.9	90.5	91.5	91.4	91.3
FSA-FiLM	99.6	89.6	84.6	78.7	77.5	77.0	76.9
GDumb-1k	91.2	85.5	85.6	83.8	76.3	78.1	79.5
GDumb-5k	99.4	99.5	99.6	98.5	99.4	98.4	99.4

Table 32. Detailed accuracy for each incremental session on **dSprites-loc** under the **high-shot CIL** setting. The best results across all methods per session are in bold while the best results across the no-memory methods are underlined. A pre-trained EfficientNet-B0 on Imagenet-1k is used as a backbone for all methods.

Method	Accuracy (%) in each session (\uparrow)									
	1	2	3	4	5	6	7	8	9	10
NA	42.0	38.0	29.9	37.0	43.9	41.3	40.7	42.4	41.2	41.2
<u>E-EWC-SDC</u>	<u>58.0</u>	<u>35.3</u>	<u>27.3</u>	<u>27.7</u>	<u>27.4</u>	<u>28.2</u>	<u>23.5</u>	<u>25.4</u>	<u>25.7</u>	<u>25.6</u>
FACT	58.7	30.6	24.9	21.4	19.1	19.0	17.6	16.9	15.5	14.7
ALICE	61.3	43.5	36.7	39.5	41.5	41.8	41.0	41.6	40.0	39.8
FSA	54.2	44.4	39.7	45.9	52.2	49.6	48.9	51.4	51.1	50.8
FSA-LL	58.0	40.5	37.0	41.6	44.3	44.9	44.9	46.1	45.1	45.4
FSA-FiLM	52.9	46.2	44.7	50.3	53.3	55.0	54.5	56.3	55.5	55.9
GDumb-1k	59.8	47.3	42.6	46.5	51.8	43.7	43.4	43.0	39.2	38.4
GDumb-5k	58.6	43.0	36.9	40.1	41.0	36.1	30.3	30.3	29.5	25.3

Table 33. Detailed accuracy for each incremental session on **FGVC-Aircraft** under the **high-shot CIL** setting. The best results across all methods per session are in bold while the best results across the no-memory methods are underlined. A pre-trained EfficientNet-B0 on Imagenet-1k is used as a backbone for all methods.

Method	Accuracy (%) in each session (\uparrow)									
	1	2	3	4	5	6	7	8	9	10
NA	72.7	49.9	49.9	46.4	47.1	47.2	44.5	44.7	44.6	43.3
<u>E-EWC+SDC</u>	<u>80.2</u>	<u>47.3</u>	<u>38.7</u>	<u>37.2</u>	<u>34.8</u>	<u>33.5</u>	<u>31.0</u>	<u>31.6</u>	<u>31.2</u>	<u>30.0</u>
FACT	79.8	2.9	1.9	1.4	1.1	0.9	0.8	0.7	0.6	0.6
ALICE	82.7	52.9	49.6	45.1	42.8	41.1	39.0	38.8	38.1	36.4
FSA	79.3	55.0	55.9	54.0	53.3	52.7	51.5	51.5	51.4	50.3
FSA-LL	81.2	49.3	50.5	49.9	49.0	46.9	46.8	46.9	46.6	45.7
FSA-FiLM	80.1	59.5	60.0	59.4	58.9	58.2	56.8	57.3	56.7	55.9
GDumb-1k	81.5	59.9	54.0	47.3	40.5	33.9	32.7	27.6	22.8	18.1
GDumb-5k	82.1	65.8	59.0	51.8	46.7	38.0	37.6	32.3	28.7	24.2

Table 34. Detailed accuracy for each incremental session on **Cars** under the **high-shot CIL** setting. The best results across all methods per session are in bold while the best results across the no-memory methods are underlined. A pre-trained EfficientNet-B0 on Imagenet-1k is used as a backbone for all methods.

Method	Accuracy (%) in each session (\uparrow)										
	1	2	3	4	5	6	7	8	9	10	11
NA	90.12	84.3	82.4	80.1	78.7	78.0	76.0	75.3	72.8	71.6	68.4
<u>E-EWC+SDC</u>	<u>99.9</u>	<u>83.4</u>	<u>64.5</u>	<u>59.9</u>	<u>47.8</u>	<u>54.1</u>	<u>42.6</u>	<u>40.4</u>	<u>31.1</u>	<u>30.0</u>	<u>33.6</u>
FACT	99.9	69.9	53.9	43.4	36.3	32.7	29.3	27.0	24.4	22.4	20.9
ALICE	99.9	96.1	93.4	89.5	88.7	87.9	85.8	83.7	81.1	79.3	75.7
FSA	99.8	96.4	94.6	91.3	90.3	89.6	87.9	86.3	83.4	82.0	78.4
FSA-LL	99.8	95.9	94.0	90.4	89.0	88.3	86.3	85.3	82.4	81.0	77.2
FSA-FiLM	99.6	96.0	94.4	92.0	91.1	90.6	88.5	87.7	85.0	83.4	79.7
GDumb-1k	96.0	92.2	89.4	86.7	85.7	83.9	81.1	80.3	76.2	75.2	70.1
GDumb-5k	99.4	98.3	97.2	95.2	94.6	94.3	92.2	91.3	88.5	86.9	82.6

Table 35. Detailed accuracy for each incremental session on **Letters** under the **high-shot CIL** setting. The best results across all methods per session are in bold while the best results across the no-memory methods are underlined. A pre-trained EfficientNet-B0 on Imagenet-1k is used as a backbone for all methods.

Method	Backbone	Accuracy (%) in each session (\uparrow)								
		1	2	3	4	5	6	7	8	9
Decoupled-Cos*	RN-20	74.6	67.4	63.6	59.6	56.1	53.8	51.7	49.7	47.7
CEC*		73.1	68.9	65.3	61.2	58.1	55.6	53.2	51.3	49.1
FACT*		74.6	72.1	67.6	63.5	61.4	58.4	56.3	54.2	52.1
FSA		75.1	71.2	67.5	63.3	60.0	57.6	55.5	54.2	52.0
NA	RN-18	68.9	65.4	62.4	58.7	57.2	54.7	53.3	51.9	50.4
FACT		75.8	71.0	66.3	62.5	59.1	56.3	54.1	51.8	49.5
ALICE \dagger		79.0	70.5	67.1	63.4	61.2	59.2	58.1	56.3	54.1
FSA-FiLM		73.0	69.7	66.3	63.2	61.9	59.3	58.3	57.2	55.2
FSA	EN-B0	82.0	78.2	74.8	70.22	68.7	66.2	65.3	63.8	61.4
NA		74.4	70.4	67.4	63.4	62.4	59.8	58.4	56.9	55.2
FACT		86.4	80.6	75.6	71.1	67.6	64.4	61.8	59.2	56.5
ALICE		87.7	83.3	78.7	74.4	72.1	69.6	67.4	65.4	62.7
FSA-FiLM	EN-B0	79.6	75.6	72.9	68.8	68.2	65.4	64.9	63.9	61.8
FSA		87.6	83.5	79.7	75.4	73.8	70.9	70.2	68.8	66.1

Table 36. Detailed accuracy for each incremental session on **CIFAR100** under the **few-shot+ CIL** setting. Asterisk (*) indicates that the reported results of a method are from [64] and \dagger that the reported results of a method are from [38]. We use three different backbones, EfficientNet-B0 (EN-B0) and ResNet-18/20 (RN-18/20); EN-B0 and RN-18 are pre-trained on Imagenet-1k.

Method	Backbone	Accuracy (%) in each session (\uparrow)										
		1	2	3	4	5	6	7	8	9	10	11
NA		70.7	66.7	63.4	59.0	58.2	56.4	54.0	52.3	50.5	50.5	50.0
Decoupled-Cos*		75.5	71.0	66.5	61.2	60.9	56.9	55.4	53.5	51.9	50.9	49.3
CEC*		75.9	71.9	68.5	63.5	62.4	58.3	57.7	55.8	54.8	53.5	52.3
FACT*	RN-18	75.9	73.2	70.8	66.1	65.6	62.2	61.7	59.8	58.4	57.9	56.9
ALICE \dagger		77.4	72.7	70.6	67.2	65.9	63.4	62.9	61.9	60.5	60.6	60.1
FSA-FiLM		72.7	68.2	64.9	60.8	60.2	58.1	55.4	54.8	53.5	53.4	52.7
FSA		76.1	72.6	69.6	65.0	64.6	62.3	61.6	59.6	58.2	58.2	57.6
NA		78.6	75.8	73.4	69.5	69.2	67.3	66.5	64.3	62.7	63.1	63.2
FACT		82.0	77.5	74.4	70.0	69.3	66.6	66.2	64.7	64.0	63.3	62.9
ALICE	EN-B0	81.6	77.1	75.1	71.9	70.5	67.8	66.8	65.7	64.1	64.0	63.5
FSA-FiLM		79.0	75.3	72.7	69.5	68.3	66.5	65.3	64.1	62.8	62.9	62.9
FSA		80.2	77.1	74.2	69.3	69.3	66.9	66.4	64.8	63.6	63.8	63.4

Table 37. Detailed accuracy for each incremental session on **CUB200** under the **few-shot+ CIL** setting. Asterisk (*) indicates that the reported results of a method are from [64] and \dagger that the reported results of a method are from [38]. We use two different backbones, EfficientNet-B0 (EN-B0) and ResNet-18 (RN-18); EN-B0 and RN-18 are pre-trained on Imagenet-1k.

Method	Accuracy (%) in each session (\uparrow)								
	1	2	3	4	5	6	7	8	9
NA	80.2 \pm 0.9	76.2 \pm 0.7	72.4 \pm 1.5	68.7 \pm 1.5	65.2 \pm 1.4	63.5 \pm 1.3	60.8 \pm 1.3	59.5 \pm 1.9	57.4 \pm 1.0
GDumb	83.9 \pm 1.4	80.1 \pm 0.5	77.6 \pm 1.6	71.7 \pm 2.2	67.5 \pm 1.8	64.0 \pm 1.5	59.4 \pm 1.2	58.6 \pm 1.9	55.7 \pm 1.0
FACT	83.0 \pm 1.2	54.5 \pm 1.4	40.7 \pm 1.0	32.6 \pm 1.0	27.6 \pm 0.9	23.8 \pm 0.7	20.8 \pm 0.5	18.7 \pm 0.4	16.8 \pm 0.3
FSA	82.7 \pm 2.1	75.4 \pm 1.7	72.5 \pm 1.8	69.5 \pm 1.6	66.8 \pm 1.8	64.5 \pm 1.4	63.1 \pm 1.5	62.7 \pm 1.5	60.3 \pm 1.3
FSA-FiLM	89.2 \pm 0.9	85.8 \pm 1.3	84.3 \pm 1.3	81.0 \pm 1.3	77.9 \pm 1.7	75.9 \pm 1.0	74.3 \pm 1.4	74.2 \pm 1.1	70.9 \pm 1.0

Table 38. Detailed accuracy for each incremental session on **CIFAR100** under the **few-shot CIL** setting. GDumb is the only memory-based method used for comparisons; we use a buffer size equal to the first session’s number of images N_1 . The best results across all methods are in bold while the best results across the no-memory methods are underlined. A pre-trained EfficientNet-B0 on Imagenet-1k is used as a backbone for all methods.

Method	Accuracy (%) in each session (\uparrow)				
	1	2	3	4	5
NA	73.5 \pm 4.6	53.3 \pm 3.7	37.3 \pm 1.8	33.6 \pm 1.5	28.3 \pm 1.1
GDumb	78.2 \pm 4.9	46.7 \pm 5.1	35.2 \pm 1.6	23.3 \pm 3.8	21.0 \pm 2.1
FACT	71.3 \pm 1.0	46.6 \pm 3.5	34.0 \pm 1.9	27.7 \pm 2.5	24.1 \pm 2.0
FSA	70.7 \pm 2.9	50.8 \pm 3.9	38.4 \pm 3.2	35.7 \pm 1.6	32.9 \pm 1.0
FSA-FiLM	90.7 \pm 1.8	70.4 \pm 1.4	60.5 \pm 1.5	55.5 \pm 2.3	51.3 \pm 2.1

Table 39. Detailed accuracy for each incremental session on **SVHN** under the **few-shot CIL** setting. GDumb is the only memory-based method used for comparisons; we use a buffer size equal to the first session’s number of images N_1 . The best results across all methods are in bold while the best results across the no-memory methods are underlined. A pre-trained EfficientNet-B0 on Imagenet-1k is used as a backbone for all methods.

Method	Accuracy (%) in each session (\uparrow)						
	1	2	3	4	5	6	7
NA	35.7 \pm 1.4	26.4 \pm 1.7	22.1 \pm 1.7	18.1 \pm 1.2	15.4 \pm 0.8	13.5 \pm 0.7	11.9 \pm 0.4
GDumb	36.4 \pm 7.9	29.9 \pm 6.3	20.3 \pm 3.6	22.1 \pm 5.5	13.1 \pm 2.1	11.7 \pm 3.2	16.4 \pm 2.6
FACT	32.6 \pm 1.4	22.7 \pm 2.2	18.4 \pm 2.1	14.4 \pm 1.9	12.4 \pm 1.5	11.9 \pm 1.6	11.7 \pm 1.7
FSA	57.4 \pm 2.3	44.8 \pm 2.8	39.3 \pm 1.6	34.8 \pm 2.1	32.9 \pm 1.9	33.2 \pm 2.6	33.7 \pm 1.7
FSA-FiLM	62.7 \pm 2.1	50.2 \pm 2.4	46.9 \pm 2.3	40.1 \pm 2.2	37.3 \pm 2.5	36.1 \pm 2.2	35.7 \pm 2.1

Table 40. Detailed accuracy for each incremental session on **dSprites-position** under the **few-shot CIL** setting. GDumb is the only memory-based method used for comparisons; we use a buffer size equal to the first session’s number of images N_1 . The best results across all methods are in bold while the best results across the no-memory methods are underlined. A pre-trained EfficientNet-B0 on Imagenet-1k is used as a backbone for all methods.

Method	Accuracy (%) in each session (\uparrow)								
	1	2	3	4	5	6	7	8	9
NA	35.5 \pm 0.9	28.7 \pm 0.7	36.4 \pm 0.8	42.8 \pm 0.4	40.0 \pm 0.4	39.4 \pm 0.6	41.4 \pm 0.7	40.3 \pm 0.9	41.0 \pm 0.7
GDumb	51.1 \pm 1.7	45.4 \pm 1.2	46.9 \pm 1.8	52.2 \pm 1.0	45.4 \pm 1.7	42.5 \pm 1.6	41.8 \pm 0.9	39.5 \pm 1.9	38.6 \pm 1.0
FACT	41.4 \pm 0.6	25.9 \pm 0.9	19.6 \pm 0.4	16.3 \pm 0.4	13.7 \pm 0.4	11.3 \pm 0.5	10.4 \pm 0.5	9.4 \pm 0.6	8.3 \pm 0.6
FSA	42.9 \pm 2.6	39.5 \pm 2.0	45.5 \pm 1.5	51.6 \pm 1.7	48.2 \pm 1.8	47.3 \pm 1.4	49.8 \pm 1.5	49.1 \pm 1.7	50.1 \pm 1.5
FSA-FiLM	46.6 \pm 1.9	44.8 \pm 1.1	49.4 \pm 0.8	52.9 \pm 1.6	54.0 \pm 0.7	53.5 \pm 1.0	55.8 \pm 0.7	55.2 \pm 0.5	55.8 \pm 0.6

Table 41. Detailed accuracy for each incremental session on **FGVC-Aircraft** under the **few-shot CIL** setting. GDumb is the only memory-based method used for comparisons; we use a buffer size equal to the first session’s number of images N_1 . The best results across all methods are in bold while the best results across the no-memory methods are underlined. A pre-trained EfficientNet-B0 on Imagenet-1k is used as a backbone for all methods.

Method	Accuracy (%) in each session (\uparrow)										
	1	2	3	4	5	6	7	8	9	10	11
NA	82.1 \pm 0.8	76.6 \pm 0.9	73.0 \pm 1.5	69.6 \pm 1.0	69.0 \pm 1.3	67.6 \pm 1.3	65.8 \pm 1.2	64.1 \pm 1.0	60.4 \pm 0.6	59.0 \pm 0.8	57.6 \pm 0.8
GDumb	91.3 \pm 1.6	91.8 \pm 1.2	80.0 \pm 1.4	72.0 \pm 1.9	69.2 \pm 3.0	63.5 \pm 1.5	59.9 \pm 1.1	54.5 \pm 0.3	48.0 \pm 0.4	44.3 \pm 1.9	41.2 \pm 1.7
FACT	84.3 \pm 1.4	72.0 \pm 1.2	68.0 \pm 2.2	63.2 \pm 1.0	62.3 \pm 1.0	59.5 \pm 1.2	58.0 \pm 1.0	55.8 \pm 1.0	52.8 \pm 0.7	51.7 \pm 0.8	49.8 \pm 0.8
FSA	87.0 \pm 1.4	79.6 \pm 1.1	76.4 \pm 0.9	72.7 \pm 0.7	73.0 \pm 0.9	71.3 \pm 0.4	69.7 \pm 0.4	68.4 \pm 0.4	64.7 \pm 0.5	62.9 \pm 0.4	62.2 \pm 0.4
FSA-FiLM	94.3 \pm 0.9	90.6 \pm 0.3	88.6 \pm 1.0	85.1 \pm 0.6	84.9 \pm 0.4	84.0 \pm 0.4	82.5 \pm 0.7	81.1 \pm 0.4	76.8 \pm 0.4	75.0 \pm 0.4	73.4 \pm 0.4

Table 42. Detailed accuracy for each incremental session on **Letters** under the **few-shot CIL** setting. GDumb is the only memory-based method used for comparisons; we use a buffer size equal to the first session’s number of images N_1 . The best results across all methods are in bold while the best results across the no-memory methods are underlined. A pre-trained EfficientNet-B0 on Imagenet-1k is used as a backbone for all methods.

Method	Accuracy (%) in each session (\uparrow)								
	1	2	3	4	5	6	7	8	9
NA	83.3 \pm 1.0	62.6 \pm 0.5	60.9 \pm 1.0	61.5 \pm 0.3	68.3 \pm 1.2	71.1 \pm 0.6	72.0 \pm 0.7	70.8 \pm 1.0	69.0 \pm 0.3
GDumb	88.3 \pm 0.4	63.6 \pm 0.8	58.6 \pm 0.6	56.4 \pm 1.0	66.0 \pm 1.1	68.7 \pm 0.4	68.9 \pm 0.6	65.8 \pm 1.0	63.2 \pm 1.1
FACT	84.3 \pm 0.6	53.6 \pm 0.6	43.0 \pm 0.5	35.9 \pm 0.6	28.3 \pm 0.6	24.2 \pm 0.3	22.6 \pm 0.3	22.0 \pm 0.5	20.6 \pm 0.2
FSA	85.2 \pm 0.3	63.3 \pm 0.3	61.4 \pm 0.7	61.6 \pm 0.5	68.5 \pm 0.9	71.2 \pm 1.1	72.2 \pm 0.5	71.2 \pm 0.7	70.3 \pm 0.4
FSA-FiLM	87.7 \pm 0.3	68.5 \pm 0.6	66.9 \pm 0.4	66.7 \pm 0.9	73.7 \pm 0.6	76.0 \pm 0.7	76.0 \pm 0.5	75.0 \pm 0.6	74.0 \pm 0.3

Table 43. Detailed accuracy for each incremental session on **DomainNet** under the **few-shot CIL** setting. GDumb is the only memory-based method used for comparisons; we use a buffer size equal to the first session’s number of images N_1 . The best results across all methods are in bold while the best results across the no-memory methods are underlined. A pre-trained EfficientNet-B0 on Imagenet-1k is used as a backbone for all methods.

Method	Accuracy (%) in each session (\uparrow)								
	1	2	3	4	5	6	7	8	9
NA	51.9	52.8	44.9	46.8	49.3	51.7	54.4	53.8	49.7
GDumb	56.4	50.1	36.3	47.5	44.2	44.7	46.4	40.9	40.4
FACT	54.9	29.9	24.6	23.8	20.4	17.8	15.7	16.4	14.3
FSA	52.1	53.6	40.0	47.8	49.2	51.3	55.1	55.1	51.5
FSA-FiLM	61.8	61.6	<u>52.0</u>	<u>56.5</u>	<u>57.0</u>	<u>59.4</u>	61.8	61.2	58.8

Table 44. Detailed accuracy for each incremental session on **iNaturalist** under the **few-shot CIL** setting. GDumb is the only memory-based method used for comparisons; we use a buffer size equal to the first session’s number of images N_1 . The best results across all methods are in bold while the best results across the no-memory methods are underlined. A pre-trained EfficientNet-B0 on Imagenet-1k is used as a backbone for all methods.